

**REPUBLIC OF TURKEY
YILDIZ TECHNICAL UNIVERSITY
GRADUATE SCHOOL OF NATURAL AND APPLIED SCIENCES**

**NATURAL CONVECTION HEAT TRANSFER FROM
VERTICALLY ARRANGED HORIZONTAL CYLINDERS**

SABRİ KALAY

**MSc. THESIS
DEPARTMENT OF MECHANICAL ENGINEERING
PROGRAM OF HEAT AND THERMODYNAMICS**

**ADVISER
ASSOC. PROF. DR. HAKAN DEMİR**

İSTANBUL, 2016

REPUBLIC OF TURKEY
YILDIZ TECHNICAL UNIVERSITY
GRADUATE SCHOOL OF NATURAL AND APPLIED SCIENCES

**NATURAL CONVECTION HEAT TRANSFER FROM
VERTICALLY ARRANGED HORIZONTAL CYLINDERS**

A thesis submitted by Sabri KALAY in partial fulfillment of the requirements for the degree of **MASTER OF SCIENCE** is approved by the committee on 02.05.2016 in Department of Mechanical Engineering, Heat and Thermodynamics Program.

Thesis Adviser

Assoc. Prof. Dr. Hakan DEMİR
Yıldız Technical University

Co- Adviser

Assoc. Prof. Dr. Ş. Özgür ATAYILMAZ
Yıldız Technical University

Approved By the Examining Committee

Assoc. Prof. Dr. Hakan DEMİR
Yıldız Technical University

Prof. Dr. Hasan HEPERKAN, Member
Yıldız Technical University

Prof. Dr. Seyhan ONBAŞIOĞLU, Member
İstanbul Technical University

ACKNOWLEDGEMENTS

I would first like to thank my thesis adviser Associate Professor Dr. Hakan Demir and co-adviser Associate Professor Dr. Şevket Özgür Atayılmaz of the Mechanical Engineering Department at Yıldız Technical University Istanbul. Their doors were always open whenever I needed their advice. I also thank Dr. Mustafa Kemal Sevindir who let me use his computer for my research.

I would also like to thank Professor Dr. Ali Cemal Benim and University of Applied Science Düsseldorf where I used the CFD laboratory in order to run simulations.

I also appreciate the support of Michael Diederich who taught me meshing and how to work with FLUENT with great patience.

Finally, I have to express my very profound gratitude to my parents for their support. Thank you.

May, 2016

Sabri Kalay

TABLE OF CONTENTS

	Page
LIST OF SYMBOLS	vii
LIST OF ABBREVIATIONS.....	vii
LIST OF FIGURES	viii
LIST OF TABLES.....	x
ABSTRACT.....	xi
ÖZET	xi
CHAPTER 1	
INTRODUCTION	1
1.1 Literature Review	1
1.2 Objective of the Thesis	10
1.3 Hypothesis	13
1.3.1 Convection Boundary Conditions	14
1.3.2 Radiation Boundary Conditions	14
1.3.3 Velocity Boundary Layer	15
1.3.4 Thermal Boundary Layer	16
1.3.5 Natural Convection and Governing Equations.....	16
1.3.6 Boundary Layer Simplified Equations.....	17
1.3.7 Prandtl Number	21
1.3.8 Grashof Number	21
1.3.9 Rayleigh Number	22
1.3.10 Nusselt Number.....	22
1.3.11 Incompressible Ideal Gas Law	23
1.3.12 Natural or Forced Convection	23
CHAPTER 2	
VERTICALLY ARRANGED CYLINDERS.....	25
2.1 Features of the Geometry	26
2.2 Mesh Independency	29
2.3 Problem Setup	31

2.3.1	General	31
2.3.2	Models	31
2.3.3	Materials	32
2.3.4	Boundary Conditions	33
2.4	Solution Methods	35
2.4.1	Pressure-Velocity Coupling	35
2.4.2	Spatial Discretization	36
2.4.3	QUICK Scheme	36
2.4.4	Power Law Scheme	37
2.4.5	Under Relaxation Factors	37
 CHAPTER 3		
	RESULTS AND DISCUSSION	40
3.1	Results for the 5 Cylinder Cases	41
3.2	First Distance Effect on Heat Transfer	46
3.3	Average Nusselt Number in the Bundle	51
3.4	Summary	55
	REFERENCES	56
 APPENDIX-A		
	HEAT TRANSFER RATES	59
	CURRICULUM VITAE	61

LIST OF SYMBOLS

A	Heat transfer area, m^2 , $A=\pi DL$
D	Cylinder diameter, m
Q _{rad}	Radiation heat loss, W
Q _{conv}	Convection heat loss, W
Q _{cond}	Conduction heat loss, W
h	Heat transfer coefficient, W/m^2k
g	Gravitational acceleration ($9.81 m/s^2$)
Ra	Rayleigh number (dimensionless),
P	Pressure (Pa)
Pr	Prandtl number (dimensionless),
T	Temperature (K)
T _s	Surface temperature (K)
T _a	Ambient temperature (K)
Nu	Nusselt number (dimensionless),
S	Center to center separation distance
R	Universal gas constant
M _w	Molecular weight of the gas
P _{op}	Operating pressure
α	Thermal diffusivity (m^2/s)
β	Thermal expansion coefficient (K^{-1})
δ	Boundary layer thickness (m)
λ	Thermal conductivity (W/m K)
ν	Kinematic viscosity (m^2/s)
θ	Tangential coordinate (rad)
ρ	Density (kg/m^3)
Δ	Difference
∞	Ambient condition
f	Mean film value
w	Wall condition

LIST OF ABBREVIATIONS

CFD	Computational Fluid Dynamics
QUICK	Quadratic Upstream Interpolation for Convective Kinematics
SIMPLEC	SIMPLE Consistent

LIST OF FIGURES

		Page
Figure 1.1	Diagram of the natural convection test facility [15].....	5
Figure 1.2	Average heat transfer coefficient for single array cylinders as a function of supply current (specific heat flux q_c) and at a fixed vertical pitch parameter $S/D = 4$ [16]	5
Figure 1.3	Average Nusselt number for upper cylinder for Rayleigh numbers from bottom to top $1.82E7$, $2.51E7$, $5.18E7$, $8.78E7$, $1.18E8$, $1.82E8$, and $2.55E8$ vs normalized cylinder center separation distance S/D [19].....	7
Figure 1.4	Average Nusselt number in array of three cylinders for (a) $Ra=1.96E7$ and (b) $Ra=5.35E7$ [22]	9
Figure 1.5	Six different cases with different number of cylinders	10
Figure 1.6	Case consisting 5 cylinders with 2D center to center equally spaced	11
Figure 1.7	Formation of the increasing distances	12
Figure 1.8	Temperatures and Rayleigh numbers, ambient temperatures (middle).....	13
Figure 1.9	Radiation boundary conditions on both surfaces of a plane wall [24]	14
Figure 1.10	The development of the boundary layer for flow over a flat plate, and the different flow regimes [24].....	15
Figure 1.11	Boundary layer showing the streamlines and separation point [28]	15
Figure 1.12	Thermal boundary layer on a flat plate (the fluid is hotter than the plate surface) [24].....	16
Figure 1.13	Typical velocity and temperature profiles for natural convection flow over a hot vertical plate at temperature T_s , inserted in a fluid at temperature T_∞ [24]	20
Figure 1.14	Isotherms in natural convection over a hot plate in air [24].....	21
Figure 1.15	Forces acting on a differential control volume in the natural convection boundary layer over a vertical flat plate [24]	21
Figure 1.16	Variation of the local Nusselt number Nu_x for combined natural and forced convection from a hot isothermal vertical plate [9]	24
Figure 2.1	One meshed cylinder, detailed look	26
Figure 2.2	Two meshed cylinder with the $S_1=3D$	26
Figure 2.3	Far look to the meshed domain	27
Figure 2.4	Quality measurement of the mesh	27
Figure 2.5	The case has 7 cylinder in an array with aspect ratio $x=1.25$	28
Figure 2.6	Selected items from the ‘Problem Setup’ from FLUENT.....	31
Figure 2.7	Selected laminar flow from FLUENT.....	32
Figure 2.8	Selected ambient fluid from FLUENT	32
Figure 2.9	Selected features of the wall.....	34
Figure 2.10	Constant temperature is chosen for the surfaces of the cylinders	34
Figure 2.11	‘top’ line of the domain	35

Figure 2.12	QUICK scheme [27].....	37
Figure 2.13	Power Law scheme [27]	37
Figure 2.14	Under Relaxation Factors	38
Figure 2.15	Residual Monitors	38
Figure 2.16	Residuals from the 2 cylinder case.....	39
Figure 2.17	Cylinders in a vertical array with the aspect ratio $x=1.1$, $T_s=323$ K, $T_a=293$ K.....	39
Figure 3.1	Aspect ratio, $x=0.8$, $S_1=10D$, 5 cylinder case, Nusselt number for each cylinder	41
Figure 3.2	Aspect ratio $x=0.9$, $S_1=10D$, 5 cylinder case, Nusselt number for each cylinder	42
Figure 3.3	Aspect ratio $x=0.95$, $S_1=10D$, 5 cylinder case, Nusselt number for each cylinder	43
Figure 3.4	Aspect ratio $x=1$, $S_1=10D$, 5 cylinder case, Nusselt number for each cylinder	43
Figure 3.5	Aspect ratio $x=1.05$, $S_1=10D$, 5 cylinder case, Nusselt number for each cylinder	44
Figure 3.6	Aspect ratio $x=1.1$, $S_1=10D$, 5 cylinder case, Nusselt number for each cylinder	45
Figure 3.7	Aspect ratio $x=1.25$, $S_1=10D$, 5 cylinder case, Nusselt number for each cylinder	45
Figure 3.8	Aspect ratio $x=0.8$ (left) and $x=1.1$ (right)	46
Figure 3.9	Nusselt numbers of 5 cylinders in a vertical array within $S_1=2D$	47
Figure 3.10	Nusselt numbers of 5 cylinders in a vertical array within $S_1=3D$	47
Figure 3.11	Nusselt numbers of 5 cylinders in a vertical array within $S_1=5D$	48
Figure 3.12	Nusselt numbers of 5 cylinders in a vertical array within $S_1=7D$	49
Figure 3.13	Nusselt numbers of 5 cylinders in a vertical array within $S_1=10D$	49
Figure 3.14	Literature comparison of the Nusselt numbers changing with S_1/D	510
Figure 3.15	Average Nusselt numbers for the bundle in different aspect ratios	51
Figure 3.16	Total convection heat transfer rate for each S_1/D case.....	52
Figure 3.17	Total heat transfer rate for each case.....	53
Figure 3.18	Total convection heat transfer rates for 5 cylinder cases	534
Figure 3.19	Convection heat transfer rates of each of 10 cylinder	54

LIST OF TABLES

	Page
Table 1.1	Max Nu and optimum wall spacing for different arrays, Ra=300 [20] 8
Table 1.2	Data from the study in order to calculate Ra and Gr numbers 24
Table 1.3	Average Nusselt number of a single cylinder and the upper of a pair of vertically aligned cylinders, with values in brackets representing the relative deviation to a single cylinder case, $(Nu - Nu_0)/Nu_0 \times 100\%$ [6] .. 25
Table 2.1	Mesh independency analysis 29
Table 2.2	Mesh characteristic of 2 cylinders case with S1=3D value under 3 different nodes values are given by Icem_Cfd mesh information..... 30
Table 3.1	Convection heat transfer rate 52
Table 3.2	Total heat transfer rate for each case 53
Table A.1	Radiation heat transfer rates for the cases 59
Table A.2	Length of the vertical array..... 60

ABSTRACT

NATURAL CONVECTION HEAT TRANSFER FROM VERTICALLY ARRANGED HORIZONTAL CYLINDERS

Sabri KALAY

Department of Mechanical Engineering

MSc. Thesis

Adviser: Assoc. Prof. Dr. Hakan DEMİR

Co-adviser: Assoc. Prof. Dr. Şevket Özgür ATAYILMAZ

Natural convection heat transfer in vertically arranged isothermal horizontal cylinders with unequal cylinder spacing in laminar flow has been investigated numerically in this thesis. The study consists of several investigations including variant numbers of cylinders as well as variant separation ratios.

Investigations were carried out with 2, 3, 4, 5, 7 and 10 center-to-center vertically arranged 4.8 mm diameter copper cylinders. Considering the bottom cylinder as the first cylinder, the distance between the first and the second cylinder (S_1) ranged as 2D, 3D, 5D, 7D and 10D, D being the outer diameter of the cylinder.

The study was carried out in 5 different low Rayleigh numbers ranging from 93 to 280. The temperature of the cylinder surfaces was set as 303 K, 313 K, and 323 K whilst the ambient and the surrounding wall's temperature was 293 K and 303 K.

The results show that increasing spacings between cylinders within a bundle enhance the heat transfer in the upper cylinders and the bundle.

Key words: Natural convection, horizontal cylinders, increasing spacings

YILDIZ TECHNICAL UNIVERSITY
GRADUATE SCHOOL OF NATURAL AND APPLIED SCIENCES

**DIKEY SIRALANMIŞ YATAY SİLİNDİRLERDE DOĞAL
TAŞINIM ISI TRANSFERİNİN GELİŞTİRİLMESİ**

Sabri KALAY

Makine Mühendisliği Anabilim Dalı

Yüksek Lisans Tezi

Tez Danışmanı: Doç. Dr. Hakan DEMİR

Eş Danışman: Doç. Dr. Şevket Özgür ATAYILMAZ

Bu çalışmada hava ortamında dikey sıralanmış yatay silindirlerde doğal taşınım ısı transferi laminer akışta sayısal olarak incelendi. Silindirler, geçmişte yapılan çalışmaların aksine, eşit aralıklarla değil, değişen aralıklarla dizildi. Farklı aralık oranlarının yanı sıra farklı sayılarda bakır boru kullanıldı.

Dikey sıralanmış silindirlerin her biri 4.8 mm çapa sahip olup, 2, 3, 4, 5, 7 ve 10 adet farklı sıralamalar simüle edilmiştir. Bu kombinasyonların yanında ilk ve ikinci borunun arası olan S_1 mesafesi, 2D, 3D, 5D, 7D ve 10D olarak 5 farklı şekilde düzenlenmiştir. D, silindir çapı olup, en alttaki silindir birinci silindir olarak adlandırılmıştır.

Sabit silindir yüzey sıcaklıkları; 303 K, 313 K, ve 323 K, ortam sıcaklıkları; 293 K and 303 K kullanılarak 93 ve 280 arasında 5 farklı Rayleigh numarasında silindirlerden yapılan ısı transferi incelenmiştir.

Sonuç olarak artan aralıklı dizilimlerde üstteki silindirlerin ısı transferi artırılarak tüm demetteki ısı transferinde iyileştirme elde edilmiştir.

Anahtar Kelimeler: Doğal taşınım, yatay silindirler, artan aralıklar

INTRODUCTION

1.1 Literature Review

In an experimental study of free convection carried out by Tillman [1] heated cylinders of 1.27 cm in diameter and 10.16 cm length, with same center-to-center horizontal and vertical spacings in the range between 1.43 cm and 3.81 cm were used. The average cylinder-to-ambient temperature was between 69 °C and 292 °C. The in-line arrays consisted of 16 cylinders while 14 cylinders were used in the staggered arrays. Tube spacing was found to have a stronger influence on the heat transfer rate than the arrangement of the array.

Farouk and Guceri [2], [3] presented a numerical analysis study of laminar and turbulent free convection from single and double, horizontal rows for both in-line and staggered arrangements of isothermal cylinders. Solutions were attained for the Rayleigh number in a range between 10^3 and 10^5 for the single row of cylinders, whilst the center-to-center horizontal spacing ranged from 2 to 6 cylinder diameters. They recorded an optimum spacing for the maximum heat transfer rate which decreased with increasing the Rayleigh number. Both, the horizontal and vertical spacings were 4 cylinder-diameters for the double rows of cylinders and the solutions were gained for the same Rayleigh numbers as for the single row of cylinders. The mean Nusselt number for the bottom cylinders was found to be nearly the same as for the single row of cylinders while the Nusselt number for the top cylinder was found to be higher than the single row. The maximum increase in average Nusselt number compared to the single cylinder was 15%, 8% and 15% for Rayleigh Numbers of 10^3 , 10^4 , and 10^5 respectively.

Steady laminar free convection from a vertical array consisting of 2–6 equally-spaced horizontal isothermal cylinders with center to center separation distances from 2 up to 50 cylinder-diameters and values of the Rayleigh number based on cylinder-diameter ranging between $5E2$ and $5E5$, set in free air, has been studied numerically through a SIMPLE-C algorithm by Corcione [4]. As a result of this study, an equation for the overall average Nusselt number for the entire array of cylinders was proposed based on the numerical results.

A numerical study containing 1-4 equally spaced horizontal isothermal cylinders was presented by Corcione [5]. In this study the horizontal and vertical spacings were ranging from 1.4 to 24 cylinder-diameters and 2 to 12 cylinder-diameters respectively. The Rayleigh number was in the range of 10^2 - 10^4 . It has been found that each investigated Rayleigh number has an optimum horizontal separation distance to diameter ratio (S/D) where the Nusselt number is at its maximum value. The average Nusselt number of any cylinder is the same as the Nusselt number of the single cylinder in large horizontal distances. As the S/D decreases, the heat transfer rate increases to the peak point due to chimney effect between the cylinders. It was found that decreasing this ratio below the optimum value reduces the heat transfer of the array due to the merging of two boundary layers. Another result of the study is that for the Rayleigh numbers mentioned before, Nusselt number of the second cylinder has decreased while the separation distance S/D was lower than 4, whereas for the 2 and 3 while it has increased at 4 and larger spacing.

Reymond et al. [6] investigated natural convection from a single cylinder and a pair of vertically arranged horizontal cylinders based on the surface heat transfer distributions of the cylinders for Rayleigh numbers of $2E6$, $4E6$ and $6E6$ with the range of cylinder spacings of 1.5, 2 and 3 diameters. According to the results for a pair of cylinders and for the ranging spacings, the heat transfer from the lower cylinder is not affected by the upper cylinder. It was found that the plume rising from the lower cylinder has a large effect on the surface heat transfer from the upper cylinder. For the spacing of 1.5 cylinder-diameter, the average Nusselt number decreased 3.8%, 8.4% and 6.5% corresponding to Rayleigh numbers $2E6$, $4E6$ and $6E6$ respectively. The combined effect of forced convection and low local temperature difference have been discussed. It has been shown that the plume rising from the lower cylinder interacts with the natural convective flow around the upper cylinder and triggers the turbulent mixing and as a

consequence enhances the mean surface heat transfer. It was clearly shown that the enhancement of the heat transfer is depending on the distance between the two cylinders.

Lieberman and Gebhart [7] carried out an experimental study on arrays of heated wires with a 0.127 mm diameter and with a Grashof number of 0.0175 in air. Comparing the wire in a vertical array with a single wire in terms of average Nusselt number showed that the Nusselt number was reduced when the distance between the wires was 37.5D. However, increasing the spacing to 75D or more, the Nusselt number of the wire in the array increased. The effect reaches the peak at around 112.5D, while it diminishes and approaches the single cylinder case in very large vertical distances.

Marsters [8] investigated natural convection heat transfer from vertically arranged heated copper cylinders in air. Heat and the spacing between the cylinders were varied. The cylinder diameter was 6.35 mm, whilst the cylinder spacing ranged from 2D to 20D. The Grashof number was in the range of 750 – 2000. Marsters presented that for closely spaced cylinders the Nusselt numbers of the cylinders in the array were reduced up to 50% compared to the single cylinder. However, for greater spacings the Nusselt numbers were increased up to 30%.

Sparrow and Niethammer [9] investigated the influence of the vertical separation distance between two horizontal cylinders with a diameter of 37.9 mm in air for Rayleigh numbers between $2E4$ and $2E5$. Distances were varied between 2D and 9D, and the best results emerged at the largest distances (8D and 9D), depending on the Rayleigh number. It was found that the Nusselt number of the upper cylinder can be improved by a factor of 1.25 compared to a single cylinder case for spacings of 6-9 diameters, whilst the distances of less than 4D diameters resulted in a reduction in the performance of the upper cylinder due to the negative effects caused by the lower cylinder plume.

Tokura et al. [10] investigated the effect of the separation distances in vertically confining walls on the heat transfer from a vertical array of 2, 3 and 5 cylinders in air for Grashof numbers from $4E4$ to $4E5$. The diameter of the cylinders was 22.3 mm, while the cylinder to cylinder distances were 1.1D, 1.5D, 2D, 3D, 7D, 10D and 15D. According to their results, the Nusselt number decreases when the distance between the cylinders is small and increases when the distance is large. Also in this research it can

be seen that confinement, by using parallel adiabatic plates, causes a chimney effect which increases the heat transfer occurring from the array.

Sadeghipour and Asheghi [11] investigated steady state free convection heat transfer from 2 to 8 horizontal cylinders in a vertical array in air at low Rayleigh numbers less than 10^3 . Their results show that for the two vertically arranged horizontal cylinders, the Nusselt number of the upper cylinder is reduced when the separation distance is less than 5 cylinder-diameter. Regarding the larger cylinder distances, the effect peaked at around 15 cylinder-diameter obtaining a 25% increase in Nusselt number.

Bejan et al. [12] carried out an experimental and numerical study on how to determine the optimal spacing between horizontal cylinders under laminar conditions. They worked up a correlation giving the optimal spacing between cylinders in a bundle based on the Rayleigh number.

Choikh et al. [13], [14] conducted a numerical investigation of natural convection heat transfer on vertically arranged horizontal cylinders in air. They arranged the cylinder spacings as $S=2D$, $3D$, $4D$, $5D$ and $6D$ for Rayleigh numbers $2E4$, $3E4$ and $4E4$. They investigated the impact of spacing and Rayleigh number on the heat transfer behavior of the cylinders. They found out that for small cylinder spacings, the Nusselt number of the upper cylinder was reduced compared to the Nusselt number of a single cylinder, whereas it was enhanced for greater spacing. Given the same spacing, the heat transfer of the top cylinder increased with the Rayleigh Number.

Persoons et al. [15] presented an experimental study consisting of a pair of isothermally heated copper cylinders with a diameter $D=30$ mm. Deoxygenated water has been chosen as the ambient fluid. The Rayleigh number and spacing effect on the heat transfer were investigated by choosing Rayleigh numbers as $1.8E6$, $3.6E$ and $5.3E6$ for the vertical spacings of $2D$, $3D$ and $4D$. The result of the experiment is that a single cylinder has no significant fluctuations of heat transfer for the used Rayleigh number range. However, in the cases of two vertically arranged horizontal cylinders having spacings from $2D$ to $4D$, it has been observed that the average heat transfer rate of the upper cylinder decreases slightly at a small spacing ($2D$) and low Rayleigh number ($1.8E6$).

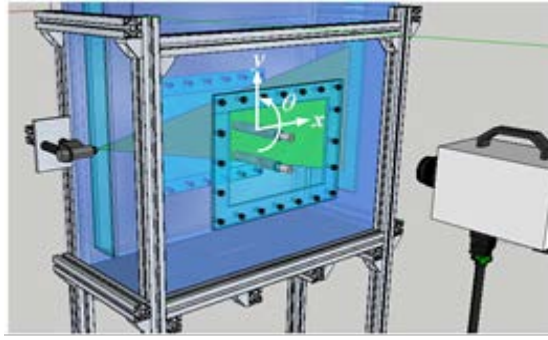


Figure 1.1 Diagram of the natural convection test facility [15]

D’Orazio and Fontana [16] investigated free convection from a pair of vertical arrays of heated horizontal cylinders set in free air. They used the Schlieren technique in order to perform heat flux and temperature measurements. For the experiments pairs of five cylinders, horizontal and vertical spacing ranging from 2 to 145 cylinder-diameter and from 4 to 12 cylinder-diameter are used respectively. The Rayleigh number was influential when the cylinder-diameter was ranging between 2.4 and 11.9. The obtained results showed that the Nusselt number of the cylinders may be enhanced or reduced depending on their spacings as well as on the Rayleigh number.

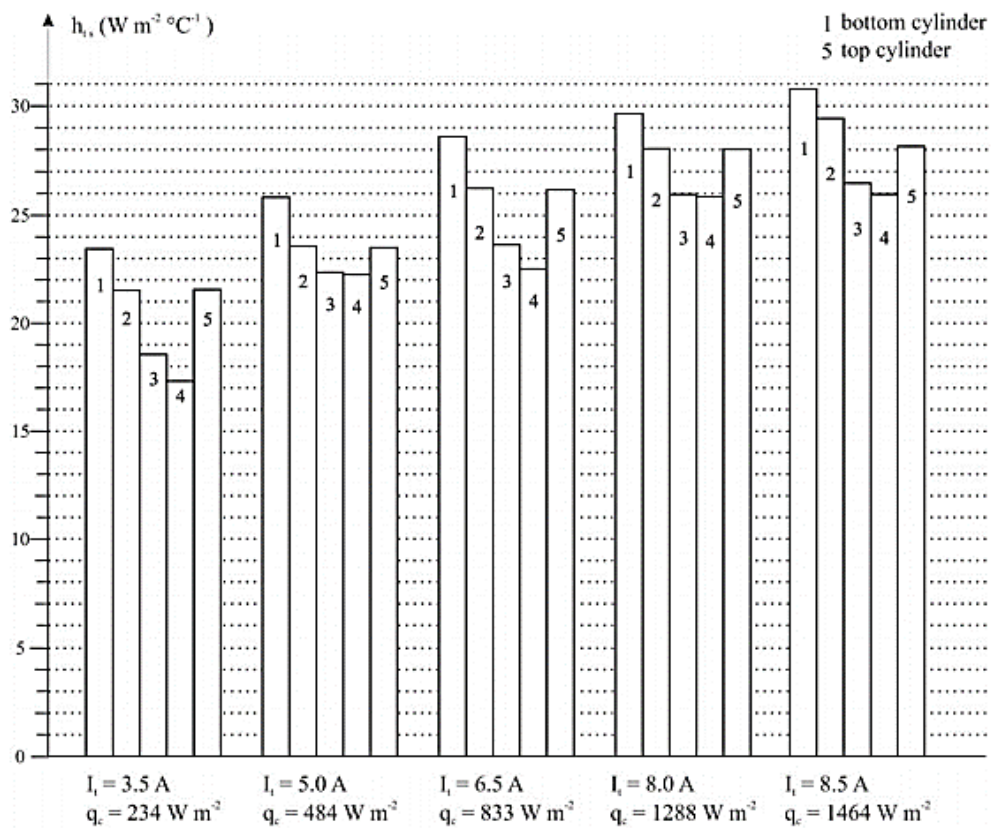


Figure 1.2 Average heat transfer coefficient for single array cylinders as a function of supply current (specific heat flux q_c) and at a fixed vertical pitch parameter $S/D = 4$ [16]

The heat transfer coefficient of the bottom cylinder can be more than 30% greater than the minimum one, which corresponds to the coefficient of the second last cylinder in the array. The heat transfer performance of the top cylinder is enhanced or decreased in comparison to the bottom tube, depending on the cylinder spacing. The bottom tube has higher values of heat transfer than the upper one for low values of S/D whereas the bottom cylinder has higher values of heat transfer for higher values of S/D .

Yuncu and Batta [17] studied the laminar flow around a vertical array of horizontal cylinders numerically and compared the results with the experimental data of Sparrow and Niethammer [18]. As the comparison results, it was found that the maximum enhancements in cylinder Nusselt number occur at around 9 cylinder-diameter.

Grafsronningen and Jensen [19] carried out an experimental study on two isothermally heated vertically aligned horizontal cylinders with a diameter of 54 mm in water. Five different separation distances used which are $S=1.5D$, $2D$, $3D$, $4D$ and $5D$ with the seven Rayleigh numbers ranging from $1.82E7$ to $2.55E8$. Regarding results, for $1.5D$ there is an increase in the average Nusselt number for $Ra=8.78E7$ or larger. For greater separation distances the increase in average Nusselt number is about 15% to 40%. They also found the optimal distance for the greatest increase in the average Nusselt number is $5D$ for $Ra=1.82E7$, $4D$ for $2.51E7$, $5.18E7$ and $8.78E7$ and $3D$ for $1.18E8$, $1.82E8$ and $2.55E8$.

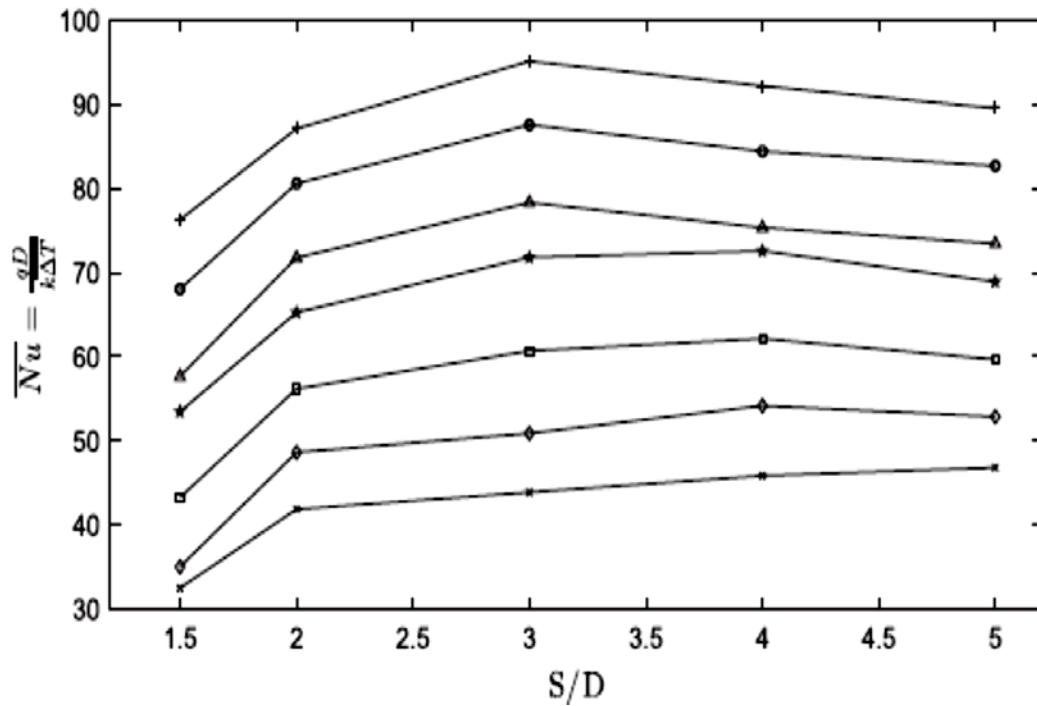
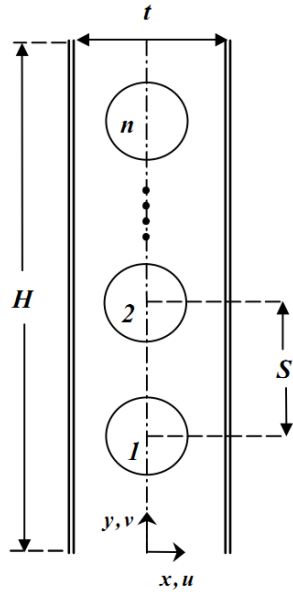


Figure 1.3 Average Nusselt number for upper cylinder for Rayleigh numbers from bottom to top 1.82E7, 2.51E7, 5.18E7, 8.78E7, 1.18E8, 1.82E8, and 2.55E8 vs normalized cylinder center separation distance S/D [19]

Hannani et al. [20] investigated the natural convection at low Rayleigh numbers from a vertical array of horizontal isothermally heated cylinders confined between two vertical walls, theoretically and numerically. They studied different numbers of cylinders and in different distances between the cylinders with varying Rayleigh numbers. The results in terms of the maximum Nusselt number and optimum cylinder spacings are carried out. It has been found out that by increasing the number of cylinders or spacings between the cylinders, the optimal spacing of the wall will be increased. However, increasing the Rayleigh number decreases the optimal spacing of the wall.

Table 1.1 Max. Nu and optimum wall spacing for different arrays, Ra=300 [20]



N	$(t/D)_{opt}$		$(\overline{Nu})_{max}$	
	$(S/D)=7$	$(S/D)=21$	$(S/D)=7$	$(S/D)=21$
2	3.1	5.5	3.35	3.58
3	3.4	6.1	3.10	3.64
4	5.4	6.6	2.82	3.66
5	6.4	7.2	2.60	3.56

As it can be seen from Figure 1.4, wall distances have less effect on the Nusselt numbers when they are increased to 21 cylinder-diameter.

Stafford and Egan [21] investigated a natural convection thermal-fluid system consisting of a heated pair of cylinders in air. They examined horizontal cylinders in both vertical and horizontal arrangement in order to define existence of optimal configurations to maximize heat dissipation at the local cylinder and in the bundle. Numerical and experimental attempts were used to evaluate cylinder interactions with the Rayleigh number ranging between 10^4 and 10^5 .

The result of their experimental study [21], the lower cylinder behaves like a single cylinder with a characteristic boundary layer thickness. The boundary layer on the bottom of the upper cylinder is thinned by the momentum of the plume arising from the lower cylinder. This is affecting the buoyancy assisted condition which enhances the local heat transfer. On the contrary, the top surface of the upper cylinder is negatively affected by the heat flow from the lower cylinder. The heat flow continues along the paths of the upper cylinder plume and results in an enlarged zone of low velocity and high temperature above the top surface of the upper cylinder. Reducing the performance locally results in both cylinders providing similar heat dissipations.

Grafsronningen and Jensen [22] investigated three vertically aligned horizontal cylinders with dissimilar cylinder spacings experimentally. Separation distances were chosen as 2D, 3D, 4D and 5D, while the Rayleigh numbers were $1.96E7$ and $5.35E7$. Turbulent mixing on the upper cylinders in the array which enhances the heat transfer is

discussed. As a conclusion of this experiment [22], the Nusselt number of the upper cylinder in the array increased compared to the lowermost cylinder. The results show that the heat exchanger may be designed with dissimilar tube spacings without a significant reduction in heat transfer from the upper cooler tubes. The reduction in cylinder spacings between the latter tubes in the upper part of the heat exchanger is attributed to turbulent effects. If the cylinder spacing between the cylinder 1 and 2 (S_1) is sufficiently large, the flow undergoes a transition from laminar to turbulent flow and the plume impinging on cylinder 2 will be turbulent. The separation distance between cylinder 2 and 3 (S_2) may be reduced compared to S_1 , it is claimed that such a configuration may contribute to a significant reduction of the heat exchangers' size compared to one designed using the optimal distance between the pair of cylinders.

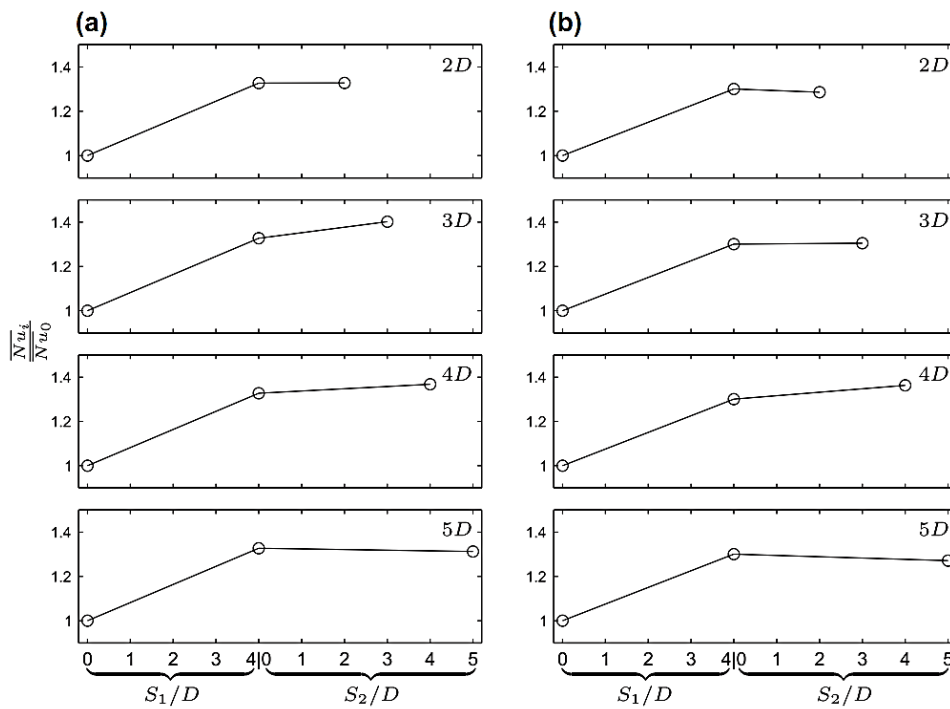


Figure 1.4 Average Nusselt number in the array of three cylinders with (a) $Ra=1.96E7$ and (b) $Ra=5.35E7$ [22]

1.2 Objective of the Thesis

The purpose of this study is to present the increasing, stable and decreasing spacing effects on the heat transfer in vertically arranged horizontal cylinders with the varying numbers of cylinders and the area cylinders cover.

Natural convection heat transfer from vertically arranged isothermal horizontal cylinders with dissimilar cylinder spacings have been investigated. The study includes different amounts of cylinders in each investigation as well as different separation ratios.

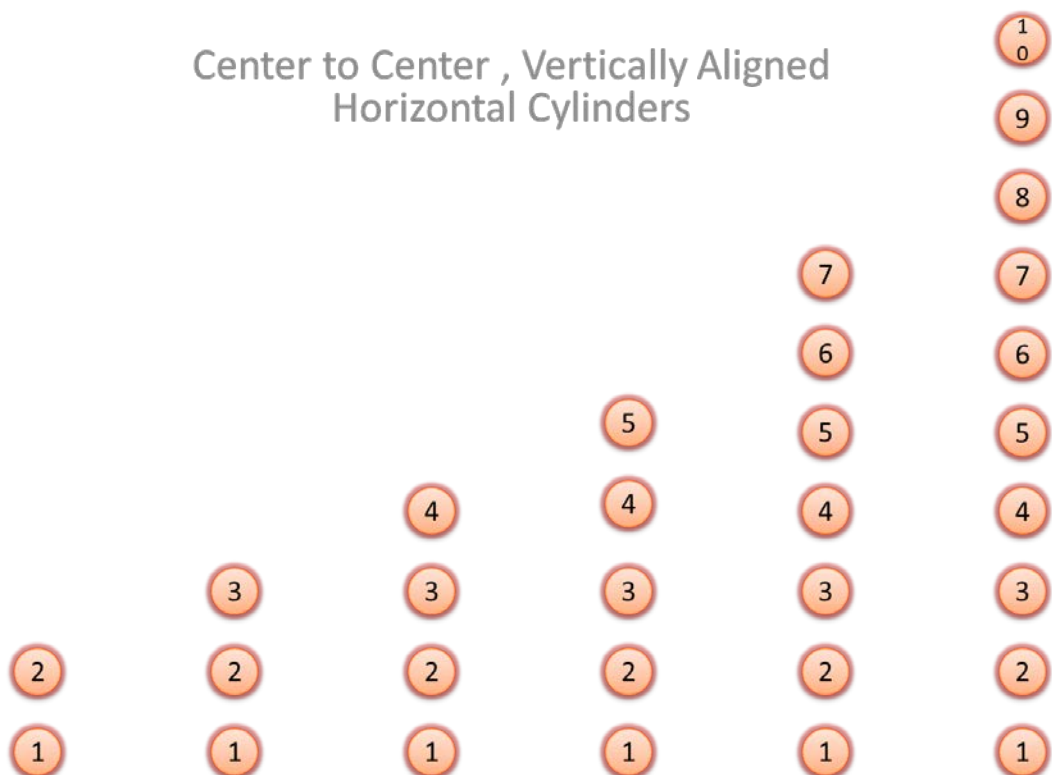


Figure 1.5 Six different cases with different numbers of cylinders

The Figure 1.5 shows the numbers of the cylinders which are studied. Investigations were carried out with 2, 3, 4, 5, 7, and 10 center-to-center vertically arranged 4.8 mm diameter copper cylinders. Considering the bottom cylinder as the first cylinder, the distance between the first and the second cylinder (S_1) ranged as 2D, 3D, 5D, 7D and 10D, D being the outer diameter of the cylinders.

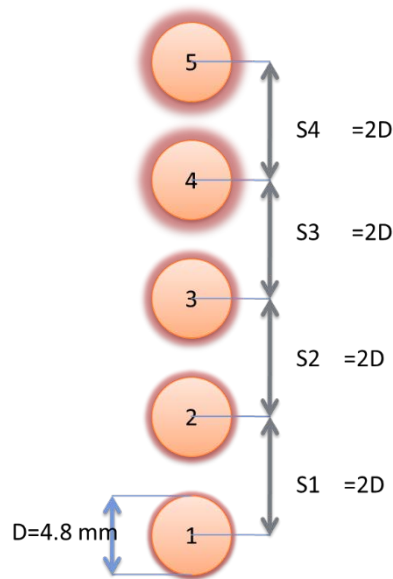


Figure 1.6 A case consisting of 5 center to center cylinders, equally spaced as $2D$

The aspect ratio (x), which describes the spacing ratio of S_N to S_{N-1} is chosen as 1.05, 1.1 and 1.25, “N” representing the total number of cylinders in the case. To give an example, in the case of 3 cylinders, S_1 is the distance between the 1st and the 2nd cylinder and S_2 is the distance between the 2nd and the 3rd cylinder. Having five different cylinder diameters of S_1 ($2D$, $3D$, $5D$, $7D$, $10D$), six different numbers of cylinders (2, 3, 4, 5, 7, 10) and three different aspect ratios ($x=1.05$, 1.1, 1.25), the total number of possible combinations is 80 (the aspect ratio does not affect the cases including only 2 cylinders). Moreover, aspect ratios of decreasing and equal distances, which are examined in order to compare, are not taken into account in this number of combinations.

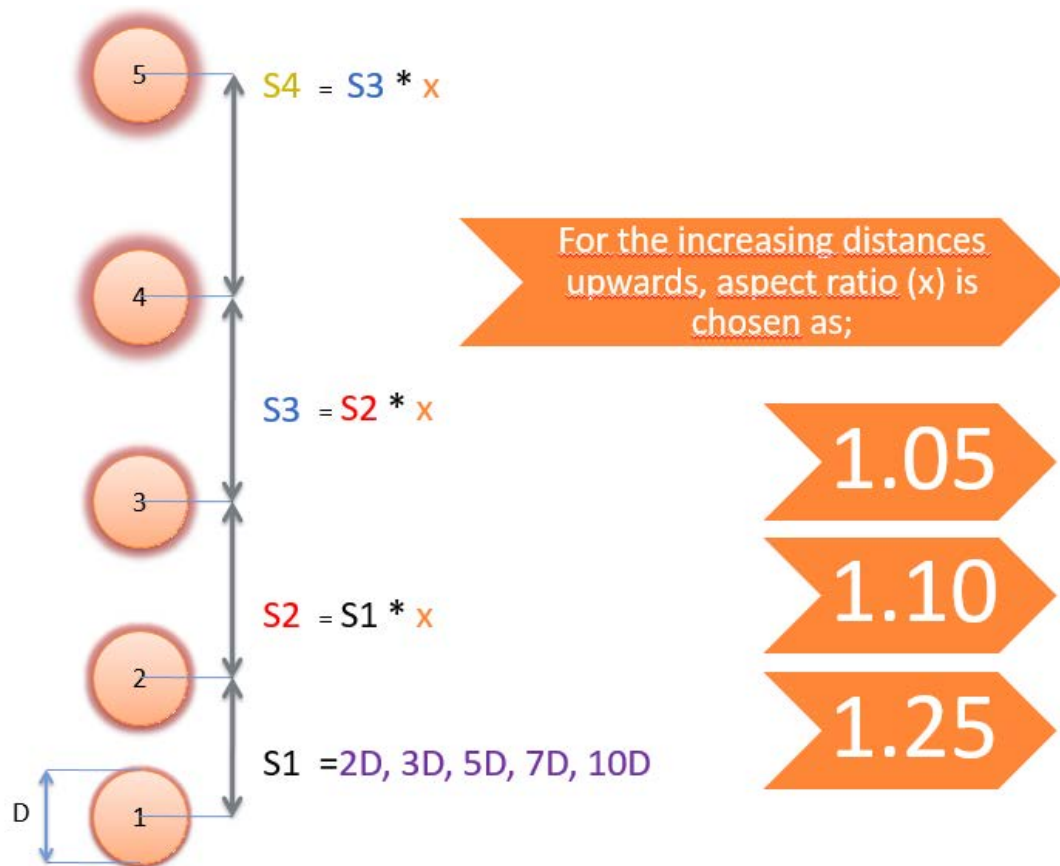


Figure 1.7 Formation of the increasing distances

In addition to these combinations, five vertically arranged cylinders with the first spacing S_1 as $10D$ are investigated more detailed in terms of different aspect ratios. In these cases, x (aspect ratio) is considered as 0.8, 0.9, 0.95, 1, 1.05, 1.1 and 1.25. The reason for adding $x < 1$ values to the study is to be able to compare the decreasing spacing effect with the increasing spacing effect in detail.

Furthermore, the cases of 10 cylinders with the S_1 value ranging as $2D$, $3D$, $5D$, $7D$ and $10D$ were numerically investigated with the $x=1$ aspect ratio in order to distinguish the effects of the increasing spacings from the constant spacings of the cylinders

The investigation was conducted in a large rectangle domain with the measurements of 2 m width and 2.2 m length while the center of the bottom cylinder was stable and it was 200 mm away from the “bottom” line of the domain. Concerning the longest vertical array which consists of 10 horizontal cylinders, $x=1.25$, $S_1=10D$, the top cylinder’s center was 760 mm away from the “top” line.

Surface, Ambient Temperatures and Rayleigh Numbers

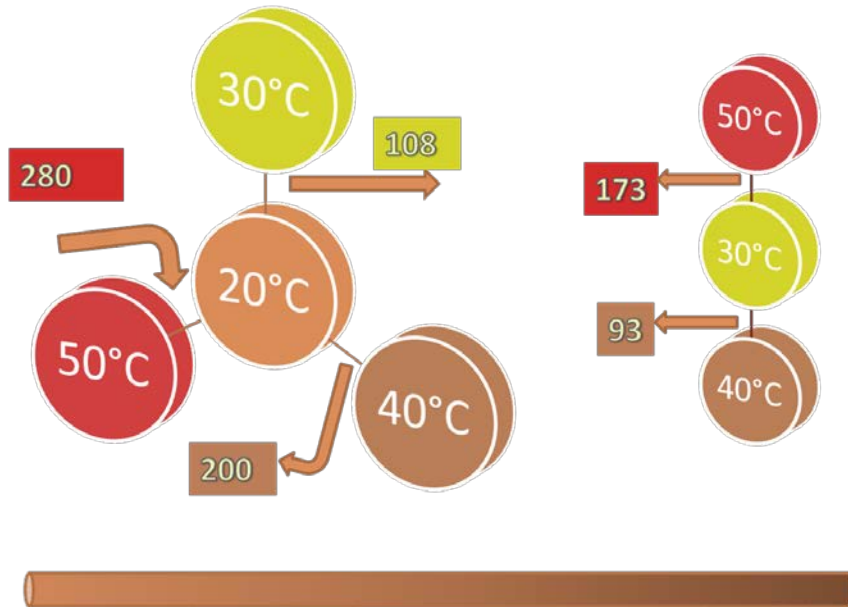


Figure 1.8 Temperatures and Rayleigh numbers, ambient temperatures (middle)

The study was carried out in 5 different low Rayleigh numbers ranging from 93 to 280. Cylinder surfaces were ranged as 303 K, 313 K and 323 K, the ambient temperature was considered as 293 K and 303 K as well as the wall surface temperatures.

Geometries of the vertically aligned horizontal cylinders have been sketched in ICEM_CFD package as well as meshes. The numerical study was performed using FLUENT package in 2D simulation.

1.3 Hypothesis

In this study, seeing the negative effect of the lower cylinder on the upper cylinders in terms of the heat transfer, it is assumed that the increasing distances between vertically arranged horizontal cylinders have great influence on the heat transfer of each cylinder and the bundle. As found out in the study of Reymond et al. [6], if the spacing between the bottom (first) cylinder and second cylinder is less than 1.5 cylinder diameter, the second cylinder diminishes the heat transfer occurring from the first cylinder at low Rayleigh numbers. For this reason, the first spacing (S_1) is set to $2D$ and more, as mentioned above.

Same distances between the cylinders in the bundle at low Rayleigh numbers also diminish the efficiency of the upper cylinders [13], [14].

Considering these facts, setting increasing distances between the cylinders in each case with different aspect ratios is assumed to result in an enhanced coefficient in terms of the convection heat transfer.

In addition, analyzing the magnitude of aspect ratio (x) as 0.8, 0.9 and 0.95, which means decreasing spacings of the cylinders in the direction of upstream, showed a dramatic decrease in the heat transfer of the cylinders.

The study presented in this paper was numerically studied using FLUENT package.

1.3.1 Convection Boundary Conditions

The convection boundary conditions for one-dimensional heat transfer in the x -direction in a plate of thickness L can be expressed as [24],

$$\begin{aligned} & \text{(heat conduction at the surface in a selected direction)} \\ & = \text{(heat convection at the surface in the same direction)} \end{aligned}$$

$$-k = \frac{\partial T(0, t)}{\partial x} = h_1 [T_{\infty 1} - T(0, t)] \quad (1.1)$$

1.3.2 Radiation Boundary Conditions

For one-dimensional heat transfer in the x -direction in a plate of thickness L ,

$$-k = \frac{\partial T(0, t)}{\partial x} = \varepsilon_1 \sigma [T_{surr, 1}^4 - T(0, t)^4] \quad (1.2)$$

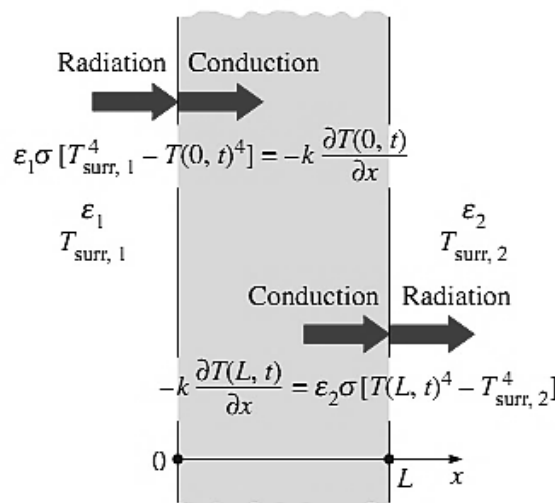


Figure 1.9 Radiation boundary conditions on both surfaces of a plane wall [24]

1.3.3 Velocity Boundary Layer

In the figure, parallel flow of a fluid over a flat plate is shown. The fluid approaches the plate in the x direction with a uniform upstream velocity of V , which is practically identical to the free stream velocity u_∞ over the plate away from the surface. This would not be the case for cross flow over blunt bodies such as cylinder [24].

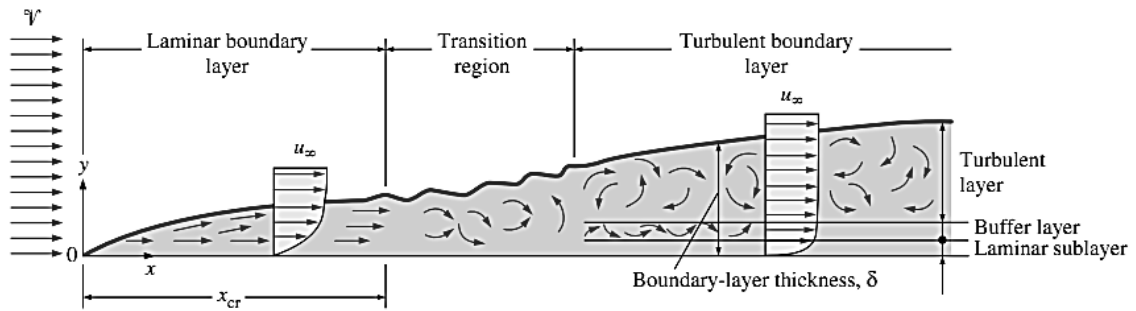


Figure 1.10 The development of the boundary layer for flow over a flat plate, and the different flow regimes [24]

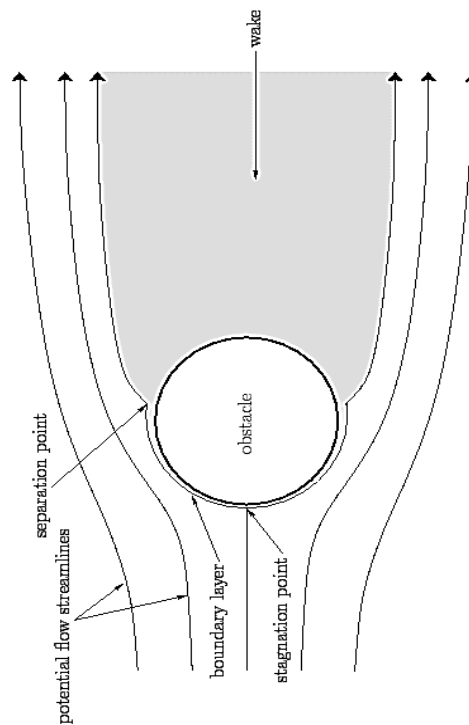


Figure 1.11 Boundary layer showing the streamlines and separation point [28]

1.3.4 Thermal Boundary Layer

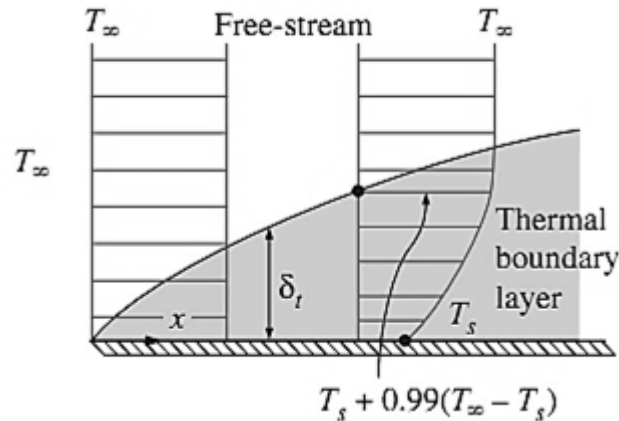


Figure 1.12 Thermal boundary layer on a flat plate (the fluid is hotter than the plate surface) [24]

A thermal boundary layer develops when a fluid at a specified temperature flows over a surface at a different temperature. When there is a flow of a fluid at a uniform temperature of T_∞ over an isothermal flat plate at temperature T_s , there will be an energy exchange between the fluid particles in the adjoining fluid layer.

The convection heat transfer rate anywhere along the surface is directly related to the temperature gradient at that location. This means, the temperature profile in the thermal boundary layer determines the convection heat transfer between a solid surface and the fluid flowing over it. In flow over a cooled surface, both velocity and thermal boundary layers will develop simultaneously. Noting that the fluid velocity has a strong influence on the temperature profile, the development of the velocity boundary layer relative to the thermal boundary layer has a strong effect on the convection heat transfer [24].

1.3.5 Natural Convection and Governing Equations

Natural convection means a heat transfer type of any flow caused by buoyancy. The convection heat transfer coefficient is a function of velocity as velocity enhances the heat transfer coefficient even though the fluid velocities of natural convection are low.

Natural convection heat transfer coefficients are very low compared to forced convection. Therefore, radiation is usually disregarded in forced convection problems, whereas it must be considered in natural convection problems that involve a gas. This is especially the case for surfaces with high emissivity. For example, about half of the heat

transfer through the air space of a double pane window is by radiation [25]. So the radiation heat transfer was taken into account in this study.

The total rate of heat transfer is determined by adding the convection and radiation components,

$$Q_{total} = Q_{conv} + Q_{rad} \quad (1.3)$$

1.3.6 Boundary Layer Simplified Equations

The formulas of continuity, momentum and energy equations are presented below [25].

x = horizontal axis

y = vertical axis

Local heat transfer coefficient h_y

$$h_y = \frac{q''_{w,y}}{T_w - T_\infty} = \frac{-k \left(\frac{\partial T}{\partial x} \right)_{x=0}}{T_w - T_\infty} \quad (1.4)$$

Continuity equation, or mass balance for steady two-dimensional flow of a fluid with constant density;

$$(m) \quad \frac{\partial u}{\partial x} + \frac{\partial v}{\partial y} = 0 \quad (1.5)$$

Momentum equations in the x and y directions;

$$(M_x) \quad \rho \left(u \frac{\partial u}{\partial x} + v \frac{\partial u}{\partial y} \right) = -\frac{\partial P}{\partial x} + \mu \left(\frac{\partial^2 u}{\partial x^2} + \frac{\partial^2 u}{\partial y^2} \right) \quad (1.6)$$

$x = 0$

$y = -\rho g$;

$$(M_y) \quad \rho \left(u \frac{\partial v}{\partial x} + v \frac{\partial v}{\partial y} \right) = -\frac{\partial P}{\partial y} + \mu \left(\frac{\partial^2 v}{\partial x^2} + \frac{\partial^2 v}{\partial y^2} \right) - \rho g \quad (1.7)$$

The energy equation for the steady two-dimensional flow of a fluid with constant properties and negligible shear stresses;

$$(Energy) \quad u \frac{\partial T}{\partial x} + v \frac{\partial T}{\partial y} = \alpha \left(\frac{\partial^2 T}{\partial x^2} + \frac{\partial^2 T}{\partial y^2} \right) \quad (1.8)$$

δ_T = The thickness of the near wall region

$$\delta_T = \left(-\frac{\partial T}{\partial x} \right)_{x=0} \sim \frac{\Delta T}{\delta_T} \quad (1.9)$$

Where, $\Delta T = T_w - T_\infty$, height y is the slender thermal boundary layer

$$\delta_T \ll y \quad (1.10)$$

Simplification of the right side of equation (1.6) through (1.7)

$$P(x, y) \cong P(y) = P_\infty(y) \quad (1.11)$$

Distribution of pressure in the reservoir is hydrostatic; therefore,

$$\frac{dP_\infty}{dy} = -\rho_\infty g \quad (1.12)$$

Due to equation (1.11) and (1.12), it has been seen that the longitudinal pressure gradient $\frac{\partial P}{\partial y}$ in the equation (1.7) replaces by the quantity $-\rho_\infty g$ where ρ_∞ is the density reservoir fluid,

$$(M) \quad \rho \left(u \frac{\partial v}{\partial x} + v \frac{\partial v}{\partial y} \right) = \mu \left(\frac{\partial^2 v}{\partial x^2} + \frac{\partial^2 v}{\partial y^2} \right) + (\rho_\infty - \rho)g \quad (1.13)$$

$$(E) \quad u \frac{\partial T}{\partial x} + v \frac{\partial T}{\partial y} = \alpha \left(\frac{\partial^2 T}{\partial x^2} + \frac{\partial^2 T}{\partial y^2} \right) \quad (1.14)$$

$$\rho = \rho(T, P)$$

$$\rho_\infty = \rho(T_\infty, P_0) \quad (1.15)$$

We obtain,

$$\rho \cong \rho_{\infty} + \left(\frac{\partial \rho}{\partial T}\right)_P (T - T_{\infty}) + \left(\frac{\partial \rho}{\partial P}\right)_T (P - P_0) + \dots \quad (1.16)$$

The pressure correction term on the right side of equation (1.14) is negligible relative to the temperature correction term;

$$\begin{aligned} \rho &\cong \rho_{\infty} - \rho_{\infty}\beta(T - T_{\infty}) + \dots \\ &\cong \rho_{\infty}[1 - \beta(T - T_{\infty}) + \dots] \end{aligned} \quad (1.17)$$

$$\rho = \rho(T, P)$$

$$1 \gg \beta(T - T_{\infty}) \quad (1.18)$$

Substituting the ρ expression (1.15) on both sides of the momentum equation,

$$\rho_{\infty}[1 - \beta(T - T_{\infty})] \left(u \frac{\partial v}{\partial x} + v \frac{\partial v}{\partial y} \right) = \mu \left(\frac{\partial^2 v}{\partial x^2} \right) + \rho_{\infty}\beta(T - T_{\infty})g \quad (1.19)$$

Looking the (1.16), $\beta(T - T_{\infty})$ term can be neglected. Dividing both sides of equation by ρ_{∞} , and writing $\nu = \mu/\rho_{\infty}$ for the kinematic viscosity of the fluid, we arrive at a momentum equation that displays T in the buoyancy term:

$$(M) \left(u \frac{\partial v}{\partial x} + v \frac{\partial v}{\partial y} \right) = \nu \left(\frac{\partial^2 v}{\partial x^2} \right) + g\beta(T - T_{\infty}) \text{ means;}$$

$$(M) \frac{v^2}{y} (\textit{inertia})$$

$$v \frac{\nu}{\delta} \frac{v}{T} (\textit{Friction}) \quad (1.20)$$

$$g\beta\Delta T (\textit{Buoyancy})$$

$$F_{net} = (\rho_{body} - \rho_{fluid})gV_{body} \quad (1.21)$$

$$F_{buoyancy} = \rho_{fluid}gV_{body} \quad (1.22)$$

The volume expansion coefficient β , defined as,

$$\beta = \frac{1}{v} \left(\frac{\partial v}{\partial T} \right)_p = \frac{1}{\rho} \left(\frac{\partial \rho}{\partial T} \right)_p \quad (1/K) \quad (1.23)$$

$$\rho\beta(T - T_\infty) = \rho_\infty - \rho \quad (\text{constant } P) \quad (1.24)$$

$$\beta_{\text{ideal gas}} = \frac{1}{T} (1/K) \quad (1.25)$$

Bejan A.[25]

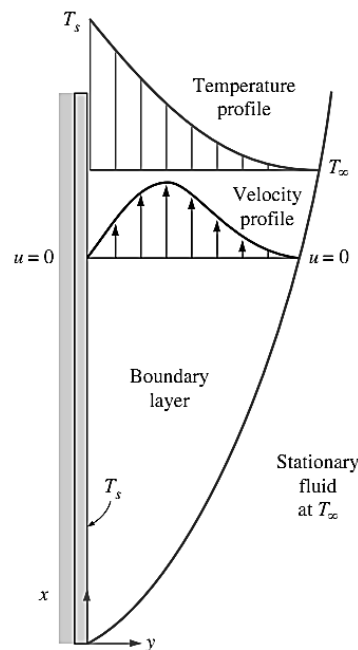


Figure 1.13 Typical velocity and temperature profiles for natural convection flow over a hot vertical plate at temperature T_s , inserted in a fluid at temperature T_∞ [24]

The higher the flow rate, the higher the heat transfer rate. The very high flow rate enhances the heat transfer coefficient magnitude in forced convection. No external forces are used in natural convection. In the case of natural convection, the flow rate is evaluated by the balance of buoyancy and friction.

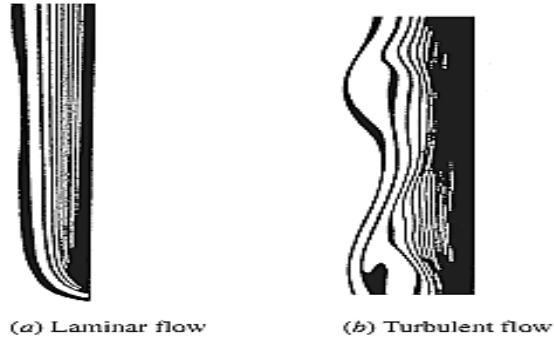


Figure 1.14 Isotherms in natural convection over a hot plate in air [24]

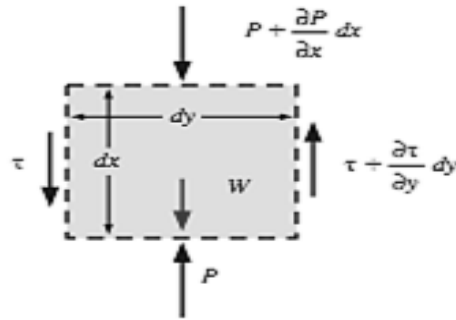


Figure 1.15 Forces acting on a differential control volume in the natural convection boundary layer over a vertical flat plate [24]

1.3.7 Prandtl Number

The relative thickness of the velocity and the thermal boundary layers is best described by the dimensionless parameter Prandtl number, defined as ratio of molecular diffusivity of momentum to molecular diffusivity of heat [24].

$$\text{Pr} = \frac{\nu}{a} = \frac{\mu C_p}{k} \tag{1.26}$$

1.3.8 Grashof Number

Concerning natural convection, the ratio of buoyancy force to the viscous force acting on the fluid is known as a dimensionless number called Grashof number. The role played by the Reynolds number in forced convection is played by the Grashof number in natural convection. Accordingly, the Grashof number provides the main criterion to determine whether the fluid flow is laminar or turbulent in natural convection [25].

For cylinders, the Grashof number is presented as,

$$Gr_L = \frac{g\beta(T_s - T_\infty)D^3}{\nu^2} \quad (1.27)$$

1.3.9 Rayleigh Number

Rayleigh number which is the product of Grashof number,

$$Ra_D = Gr_L \cdot Pr = \frac{g\beta(T_s - T_\infty)D^3}{\nu^2} \cdot Pr \quad (1.28)$$

Based on the local altitude y is presented as,

$$Ra_y = \frac{g\beta(T_w - T_\infty)y^3}{\alpha\nu} \quad (1.29)$$

1.3.10 Nusselt Number

The Nusselt number is named after Wilhelm Nusselt, who made significant contributions to convective heat transfer and it is viewed as the dimensionless convection heat transfer coefficient.

The natural convection flow around an isothermal cylinder positioned horizontally in a fluid reservoir is similar to the flow along a vertical surface. The only difference is that now the wall is curved, and instead of the wall height y the vertical dimension is the cylinder diameter D . These similarities explain why the heat transfer correlation for horizontal cylinders has the same form as the vertical wall correlation. The equation is valid for ($10^{-5} < Ra_D < 10^{12}$) and the entire Prandtl number range. The average Nusselt number and the Rayleigh number are both based on the diameter for horizontal cylinders. The following correlations are recommended by Churchill and Chu [26]:

$$\overline{Nu}_D = \left\{ 0.6 + \frac{0.387 Ra_D^{\frac{1}{4}}}{\left[1 + \left(\frac{0.559}{Pr} \right)^{\frac{9}{16}} \right]^{\frac{8}{27}}} \right\}^2 \quad (1.30)$$

Heat transfer through the fluid layer is by convection when the fluid involves some motion and by conduction when the fluid layer is motionless. Heat flux (the rate of heat transfer per unit time per unit surface area) in either case is,

$$q_{conv} = h\Delta T \quad (1.31)$$

$$q_{cond} = \frac{k\Delta T}{L} \quad (1.32)$$

$$\frac{q_{conv}}{q_{cond}} = \frac{hL}{k} = Nu \quad (1.33)$$

1.3.11 Incompressible Ideal Gas Law

In Ansys Fluent, if the density is chosen using the ideal gas law for an incompressible flow, the solver computes the density as,

$$\rho = \frac{P_{op}M_w}{RT} \quad (1.34)$$

1.3.12 Natural or Forced Convection

The convection heat transfer coefficient is a function of the fluid velocity whether it is natural or forced convection. It is stated clearly in the literature that natural convection is always combined with forced convection. While ignoring the velocity in the natural convection, this error is negligible at high velocities whereas ignoring the forced convection requires low velocities in order to be neglected. Hence, obtaining a criterion to evaluate the relative magnitude of the forced convection in the natural convection is necessary.

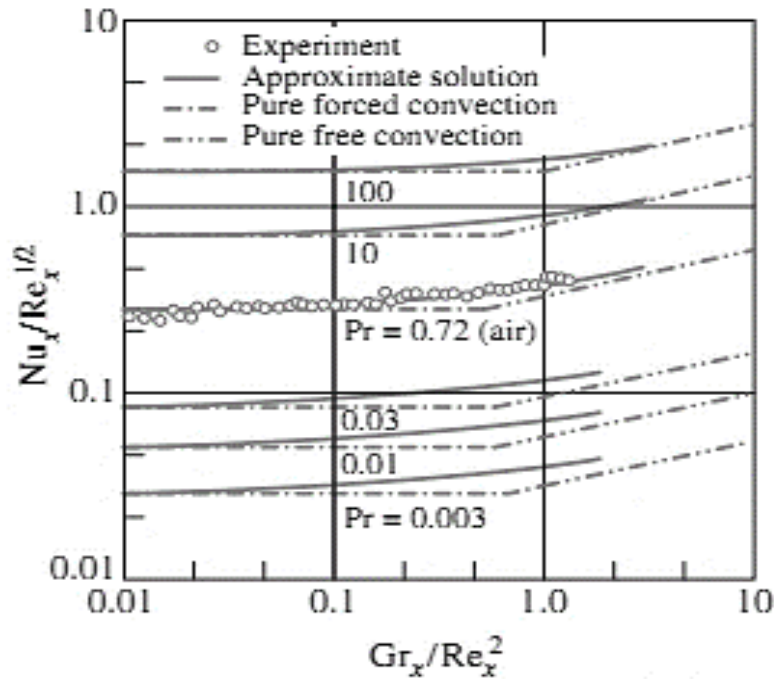


Figure 1.16 Variation of the local Nusselt number Nu_x for combined natural and forced convection from a hot isothermal vertical plate (Lloyd and Sparrow) [9]

As shown in the figure, forced convection is negligible in air when $Gr/Re^2 > 1$.

Table 1.2 Data from the study in order to calculate Ra and Gr numbers

D=	0,0048	m
T_s=	323	K
T_a=	293	K
T_f=	308	K
g=	9,81	m/s ²
β=	0,003246753	1/K(T _f)
Pr=	0.7255	
ν=	1.702*10 ⁻⁵	m ² /s
Ra=	280.4	
Gr=	386.49	

The Grashof number is found as 386.49 when the Rayleigh number is 280, due to the equation (1.27) as the Table 1.2 above shows. The Grashof number can be considered as the Reynold number in natural convection. When the Reynold number is taken into consideration the velocity is dictated by external forces which means by existence of the forced convection.

In this perspective, forced convection is found to be negligible in this study.

VERTICALLY ARRANGED CYLINDERS

In previous works, Kazemzadeh et al. [20], it has been shown that the heat transfer characteristics of a pair of aligned horizontal cylinders are significantly different from those of a single cylinder. Reymond et al. [6] have carried out that only when both cylinders are heated, a considerable degree of interaction occurs in the surface heat transfer rate from the upper cylinder. For a spacing of 1.5D or more, the lower cylinder is unaffected by the upper cylinder.

Table 2.1 Average Nusselt number of a single cylinder and the upper of a pair of vertically aligned cylinders, with values in brackets representing the relative deviation to a single cylinder case, $(Nu - Nu_0)/Nu_0 \times 100\%$ [6]

	$Ra = 1.8 \times 10^6$	$Ra = 3.6 \times 10^6$	$Ra = 5.3 \times 10^6$
Single cylinder ($S = \infty$)	$Nu = 16.9$	$Nu = 20.7$	$Nu = 23.8$
Upper cylinder ($S = 4D$)	$Nu = 18.0$ (+6.1%)	$Nu = 22.8$ (+9.2%)	$Nu = 24.3$ (+2.0%)
Upper cylinder ($S = 3D$)	$Nu = 18.2$ (+7.2%)	$Nu = 22.4$ (+7.6%)	$Nu = 26.5$ (+10.2%)
Upper cylinder ($S = 2D$)	$Nu = 16.1$ (-5.1%)	$Nu = 22.3$ (+7.2%)	$Nu = 24.5$ (+3.1%)

2.1 Features of the Geometry

The lengths of the geometries are given in the Appendix A. It shows the height of the bundle for each case depending on the cylinders' locations and coordinates. Despite the coordinate origin being the lowermost cylinder's center, the bottom of the first cylinder is considered as the beginning point when measuring the height of the bundle.

Investigations were carried out with 2, 3, 4, 5, 7 and 10 center-to-center vertically arranged copper cylinders of 4.8 mm diameter. The bottom cylinder is called the first cylinder. The distance between the first and second cylinder (S_1) is ranged as 2D, 3D, 5D, 7D and 10D.

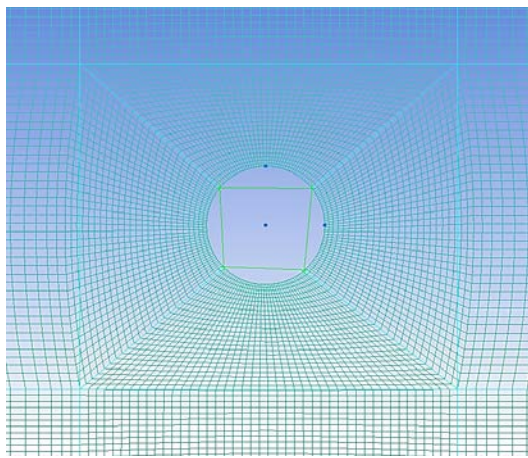


Figure 2.1 One meshed cylinder, detailed look

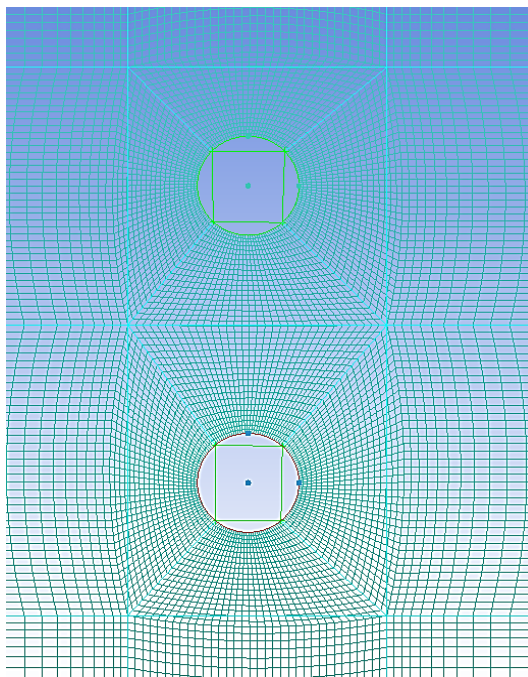


Figure 2.2 Two meshed cylinder with the $S_1=3D$

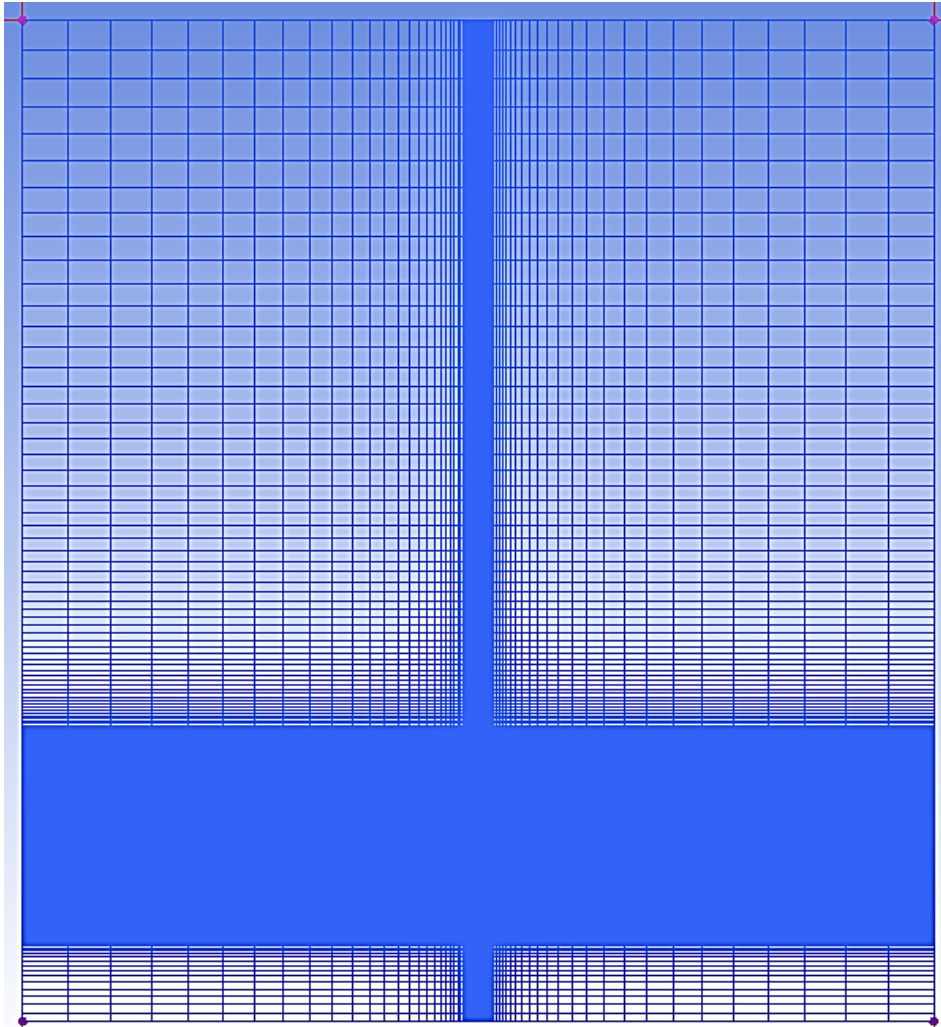


Figure 2.3 Far look to the meshed domain

Figure 2.3 shows a photo of the meshed domain from the Icem_CFD. The cylinders are invisible in the photo due to the very small cylinder diameter (4.8 mm) compared to the whole domain.

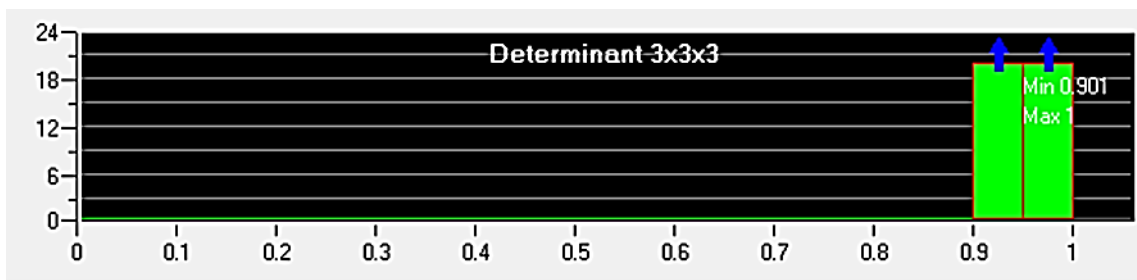
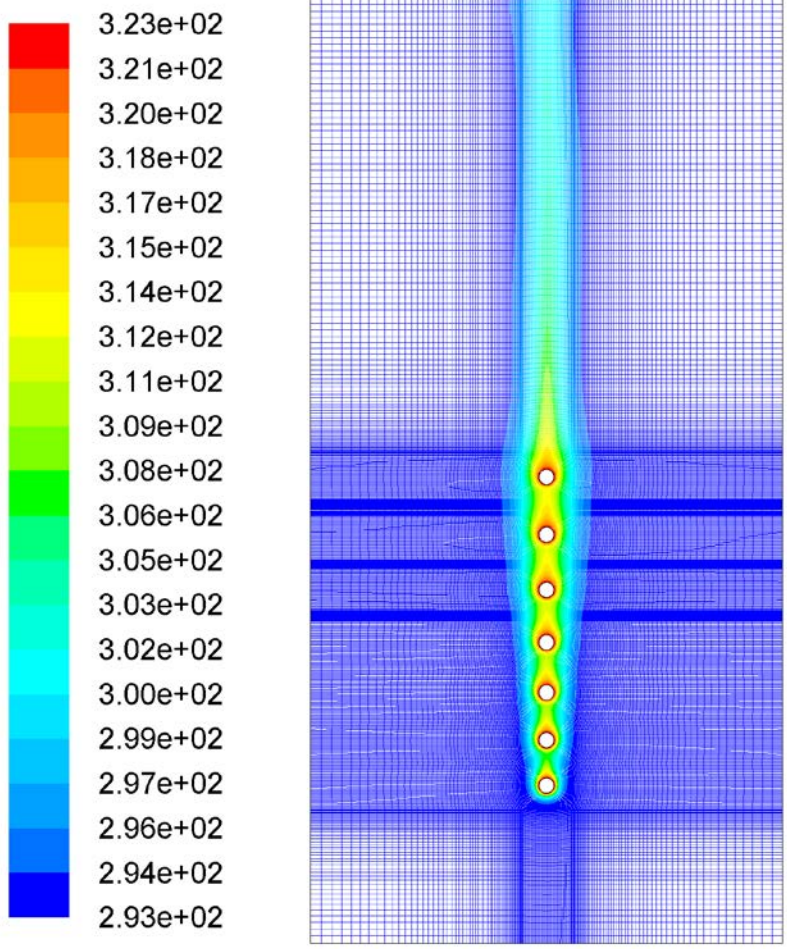


Figure 2.4 Quality measurement of the mesh



Contours of Static Temperature (k)

Jun 17, 2015
ANSYS FLUENT 13.0 (2d, pbns, lam)

Figure 2.5 Seven cylinder case in an array with aspect ratio $x=1.25$

2.2 Mesh Independency

The meshes were generated by usage of the Icem_CFD package. The sketched domain consists of quadrilateral computational mesh. Mesh independence has been examined for the cases within 1, 2, 3, 7, and 10 vertically arranged horizontal cylinders.

Table 2.2 Mesh independency analysis

Cylinders	Total Nodes	Total heat transfer, q	$(q-q_{ref})/q_{ref}$
1 cylinder	17244	7.32 W	0.0237
	(ref)44708	7.15 W	-
	94460	7.17 W	0.00279
2 cylinders $S_1=3D$	32272	12.2 W	0.025
	(ref)46952	11.9 W	-
	157856	12.1 W	0.016
3 cylinders $x=1.1$ $S_1=3D$	45428	17.77 W	0.056
	(ref)65328	18.53 W	-
	112188	18.64 W	0.005
7 cylinders $x=1.1$ $S_1=10D$	(ref)62302	57.53 W	-
	196378	56.23 W	0.022
10 cylinders $x=1.25$ $S_1=10D$	161248	87.70 W	0.0018
	(ref)264844	87.86 W	-
	388564	87.89 W	0.00034

Table 2.3 Mesh characteristics of the 2 cylinder case with $S_1=3D$ under 3 different node numbers are given by Icem_Cfd mesh information

Information of Total Elements:				
Total Elements	Total Nodes	LINE_2	NODE	QUAD_4
47540	46951	1168	4	46368

Information of Individual Part:		
Part Name	Number of Elements	Number of Nodes
BOTTOM	152	153
CIRCLE1	146	146
CIRCLE2	146	146
CREATED_FACES	0	0
FLUID	46368	46951
LEFT	286	287
POINT	4	4
RIGHT	286	287
TOP	152	153

Information of Total Elements:				
Total Elements	Total Nodes	LINE_2	NODE	QUAD_4
330026	328312	3418	4	326604

Information of Individual Part:		
Part Name	Number of Elements	Number of Nodes
BOTTOM	407	408
CIRCLE1	636	636
CIRCLE2	596	596
CREATED_FACES	0	0
FLUID	326604	328312
LEFT	686	687
POINT	4	4
RIGHT	686	687
TOP	407	408

Information of Total Elements:				
Total Elements	Total Nodes	LINE_2	NODE	QUAD_4
158910	157806	2198	4	156708

Information of Individual Part:		
Part Name	Number of Elements	Number of Nodes
BOTTOM	317	318
CIRCLE1	336	336
CIRCLE2	316	316
CREATED_FACES	0	0
FLUID	156708	157806
LEFT	456	457
POINT	4	4
RIGHT	456	457
TOP	317	318

In order to gain more accurate results, instead of considering the whole area, different numbers of nodes in the cylinder area are calculated and compared.

2.3 Problem Setup

2.3.1 General

All simulations were completed under the ‘double precision’ solver and with two-dimensional simulation in FLUENT. Referring to the ‘FLUENT User’s Guide’, double precision solver was used for all cases to get more accurate results in terms of heat transfer in the system.

As shown in Figure 2.6, ‘Pressure-Based’ solver was used with absolute velocity formulation in steady state conditions during the calculations. Due to the natural convection problem, only the gravity was counted in the direction of the minus Y axis.

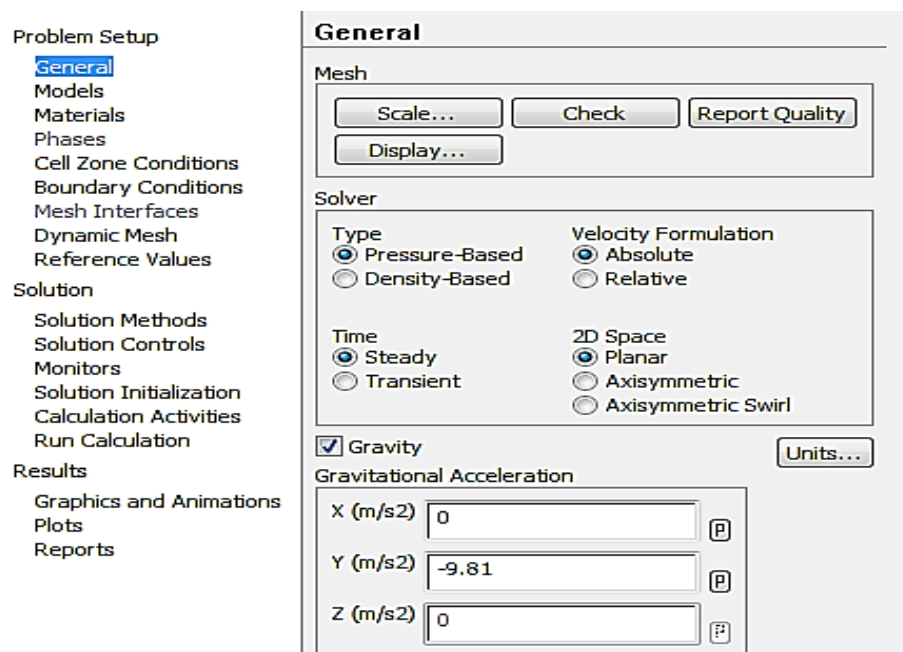


Figure 2.6 Selected items from the ‘Problem Setup’ in FLUENT

2.3.2 Models

As shown in Figure 2.7, the energy equation was set to ‘on’, and ‘Laminar viscous’ flow was chosen due to natural convection.

In order to take the radiation heat transfer into account, it was activated and radiation model was selected as ‘Surface to Surface’.

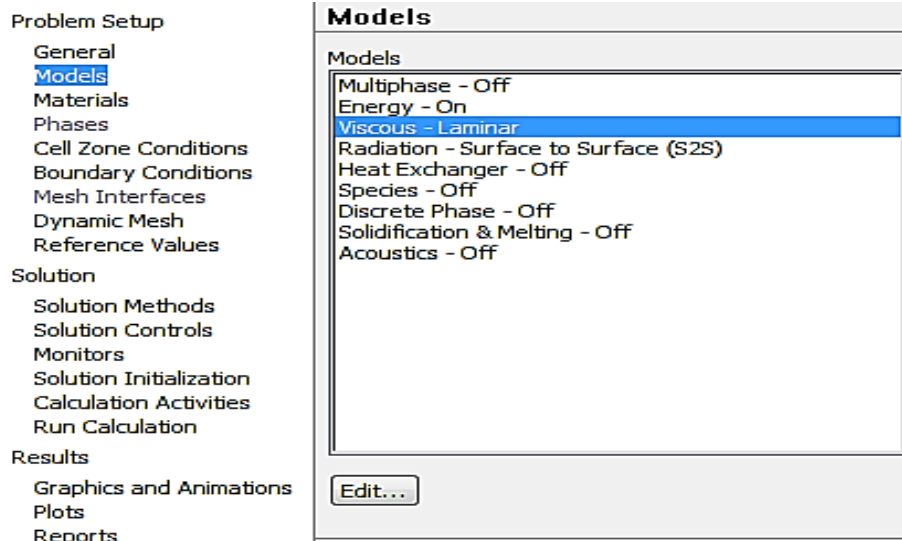


Figure 2.7 Selected laminar flow in FLUENT

2.3.3 Materials

Air is used as ambient fluid and its temperature was set at 20°C and 30°C. It is presumed as ‘incompressible ideal gas’.

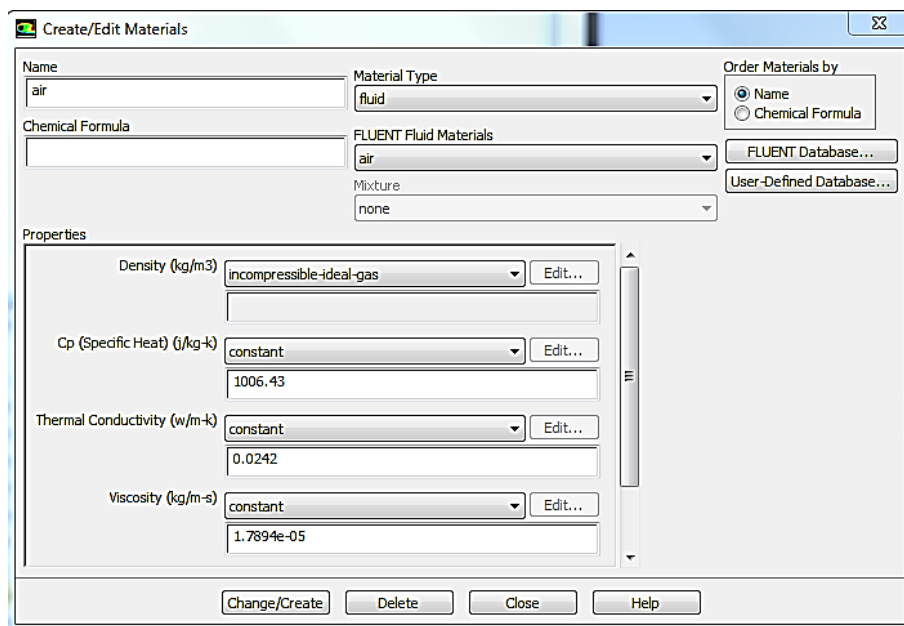


Figure 2.8 Selected ambient fluid from FLUENT

The solid components of the study are the cylinders made of copper and the walls made of aluminium.

2.3.4 Boundary Conditions

2.3.4.1 Wall Boundary Conditions

Even though a large domain was sketched in the study, some boundary conditions were defined to limit the domain. While the upper line has been set as ‘pressure inlet’ condition with the name of ‘TOP’ line, the rest of the domain boundaries were defined as ‘wall’ conditions with the name of ‘LEFT’, ‘RIGHT’ and ‘BOTTOM’ depending on the position. The material of these surrounding walls was chosen as aluminum whereas the cylinders’ material was copper. The surfaces of the cylinders were also set as ‘wall’ boundary.

Fixed temperature conditions were applied to the walls and the heat flux was found by the defined equation:

$$q = h_f(T_w - T_f) + q_{rad} \quad (2.1)$$

For the outer surfaces of the cylinders, the temperature was set at 323 K, where the fluid and the surrounding wall temperature was 293 K for the case in which the Rayleigh number corresponds to 280.

The walls surrounding the domain were defined as ‘adiabatic wall’ and therefore the heat flux was taken as ‘0’.

The fluid-side heat transfer at the walls in laminar flows was computed using Fourier’s law.

$$q = k_f \left(\frac{\partial T}{\partial n} \right)_{wall} \quad (2.2)$$

n is the local coordinate normal to the wall

For all wall conditions, ‘Stationary Wall’ option was chosen. Beside this, ‘No Slip’ option was chosen for the shear condition.

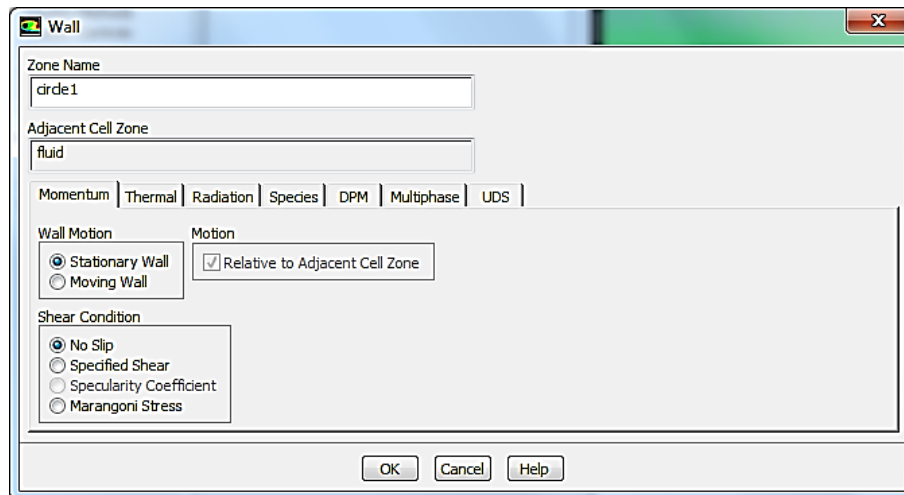


Figure 2.9 Selected features of the wall

Cylinders were named ‘circle’ in the study as can be seen in Figure 2.9. For all cylinders, the emissivity was set to 0.5 due to radiation heat transfer.

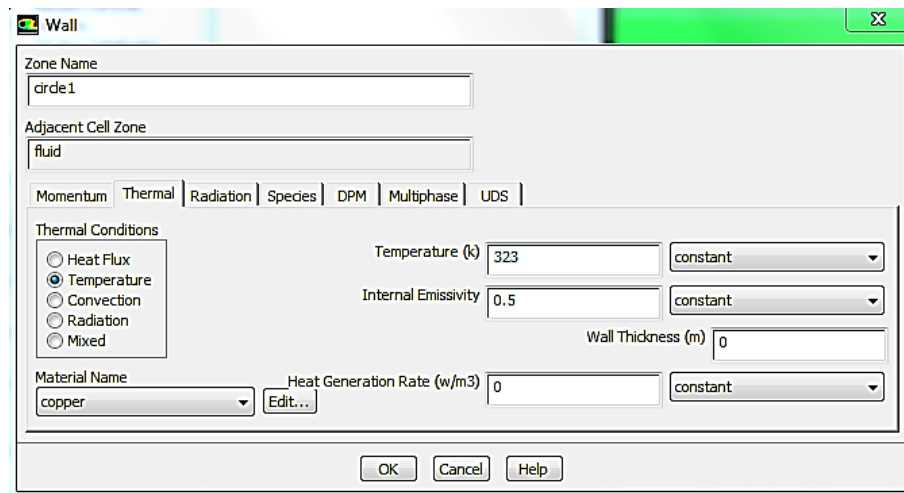


Figure 2.10 Constant temperature is chosen for the surfaces of the cylinders

2.3.4.2 Pressure Inlet Boundary Conditions

The treatment of the pressure inlet boundary conditions in FLUENT is described as loss-free transition from stagnation conditions to the inlet conditions in its tutorial.

For incompressible flows, this transition is attained by applying the Bernoulli equation to the inlet boundary. For incompressible flows, the equivalent isentropic flow relations for an ideal gas are used.

The total pressure for an incompressible fluid is defined as

$$\rho_0 = \rho_s + \frac{1}{2} \rho \overline{|\vec{v}|^2} \quad (2.3)$$

$\rho_0 = \text{total pressure}$, $\rho_s = \text{static pressure}$

When the flow exits through the pressure inlet, the total pressure specified is used as the static pressure. For incompressible flows, total temperature is equal to static temperature.

In the cases presented in this paper, ‘TOP’ line boundary condition was set to ‘pressure inlet’ boundary conditions. As a pressure value, Gauge pressure was set to “0” which is equal to atmospheric pressure. Besides this, the internal emissivity for the radiation heat transfer was set to ‘0.85’ for the lines of ‘TOP’, ‘RIGHT’, ‘LEFT’ and ‘BOTTOM’.

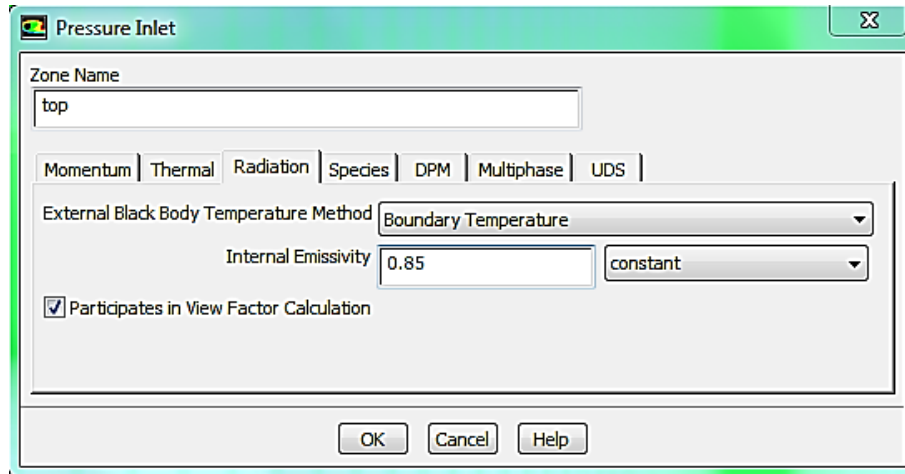


Figure 2.11 ‘top’ line of the domain

2.4 Solution Methods

2.4.1 Pressure-Velocity Coupling

Pressure-velocity coupling refers to a numerical algorithm and uses a combination of continuity and momentum equations to derive an equation for pressure (or pressure correction) when using the pressure-based solver.

2.4.2 Spatial Discretization

To be able to get the best results from FLUENT package, a couple of different solution methods have been applied. Because of achieving the best results regarding converge issue, the following methods were chosen:

“Least Squares Cell Based” discretization was chosen as Gradient. For the pressure, “Body Force Weighted” was chosen and for momentum and energy equations, “Power Law” solution method was used, although “QUICK Scheme” and “First Order” methods had been tried before.

Even though “First Order” discretization allowed to get results, to have precise results, the more accurate method “Power Law” was applied. “QUICK Scheme” method was also applied but it resulted in some converge problems when it was applied to the geometrically complicated cases.

2.4.3 QUICK Scheme

QUICK stands for Quadratic Upwind Interpolation for Convective Kinetics. A quadratic curve is fitted through two upstream nodes and one downstream node.

From the numerical schemes, the shape of the function ‘ ϕ ’ can be assumed. This function can be approximated by Taylor series polynomials [27]:

$$\phi(x_e) = \phi(x_p) + \frac{\phi'(x_p)}{1!}(x_e - x_p) + \frac{\phi''(x_p)}{2!}(x_e - x_p)^2 + \dots + \frac{\phi^n(x_p)}{n!}(x_e - x_p)^n + \dots \quad (2.4)$$

The central differencing scheme and second order upwind scheme do include the first order derivative, but ignore the second order derivative. These schemes are therefore considered second order accurate. QUICK does take the second order derivative into account, whereas ignores the third order derivative. This is then considered third order accurate.

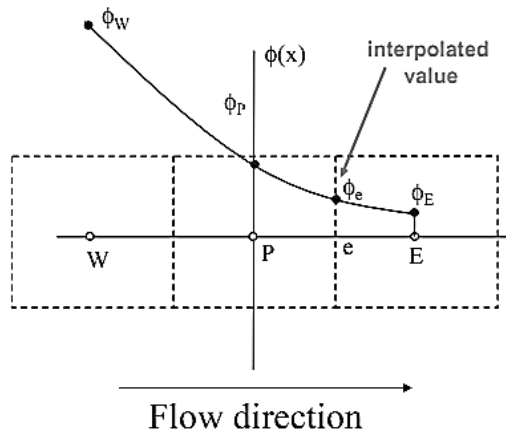


Figure 2.12 QUICK scheme [27]

2.4.4 Power Law Scheme

The Power Law Scheme is based on the analytical solution of the one-dimensional convection-diffusion equation. The face value is determined from an exponential profile through the cell values. The exponential profile is approximated by the following power law equation [27]:

$$\phi_e = \phi_p - \frac{(1-0.1Pe)^5}{Pe} (\phi_e - \phi_p) \quad (2.5)$$

Pe is the Peclet number. For $Pe > 10$, diffusion is ignored and first order upwind is used.

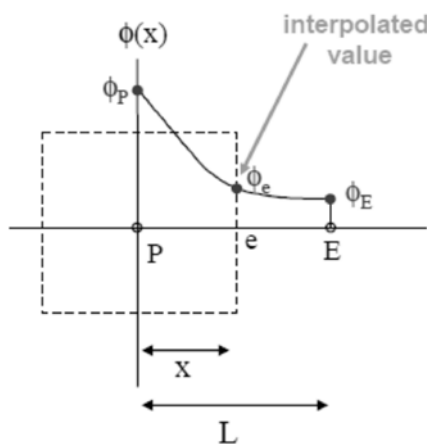


Figure 2.13 Power Law scheme [27]

2.4.5 Under Relaxation Factors

The values under relaxation factors were applied as indicated in Figure 2.14 below to obtain the aimed values of convergence. Differing from the “Default” settings of the

software, only the momentum value was changed to 0.1 from 0.7. The values are presented in the figure below.

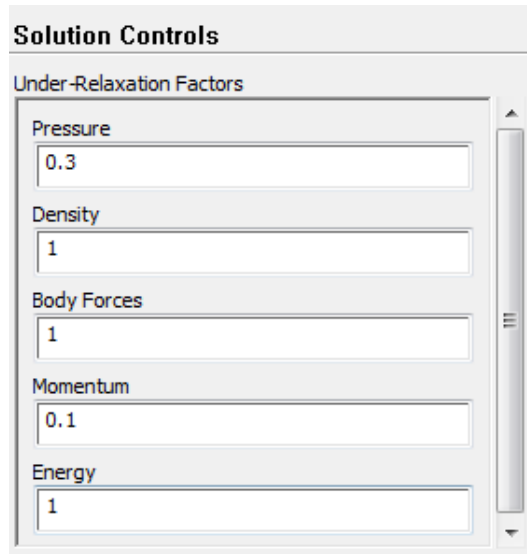


Figure 2.14 Under Relaxation Factors

In order to keep the residual instabilities at minimum and to obtain better results, after running the cases with the absolute criteria of 10^{-3} in terms of continuity, x-velocity, y-velocity and energy equations, the residuals were changed to 10^{-4} .

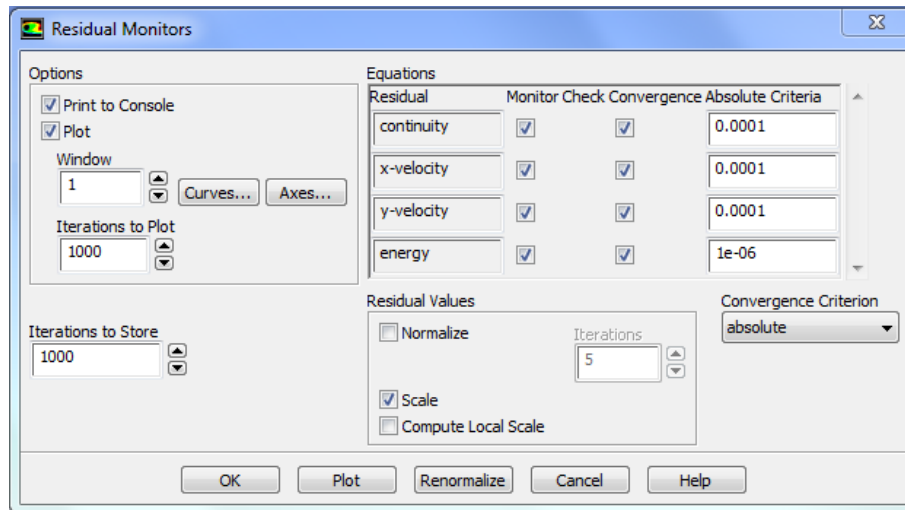


Figure 2.15 Residual Monitors

The figure below shows the residual graph example of the case ($S_1=5D$, $x=1.1$, 10 pipes). As can be seen from the sample, convergence was gained at around 3800 iterations.

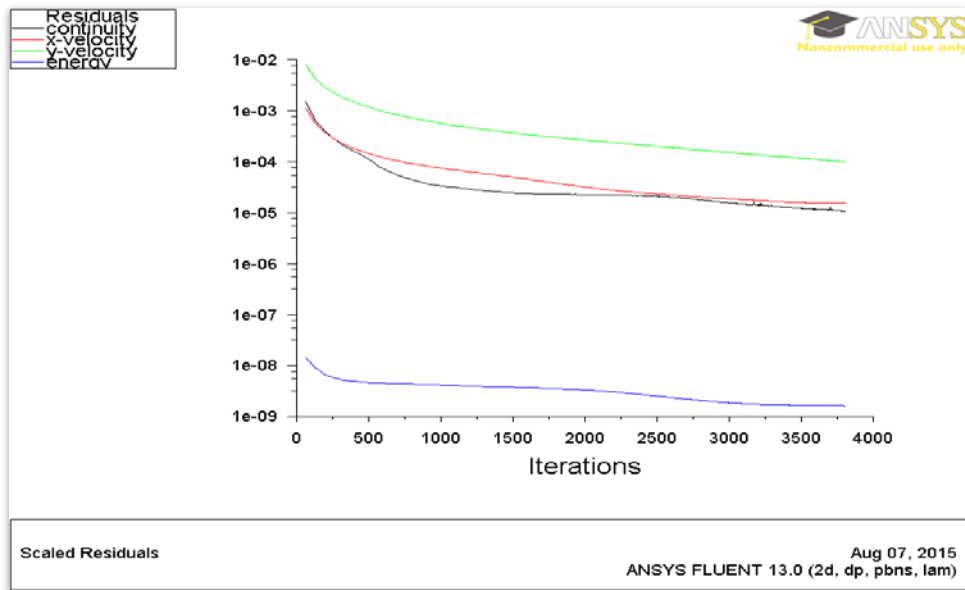


Figure 2.16 Residuals of the 2 cylinder case

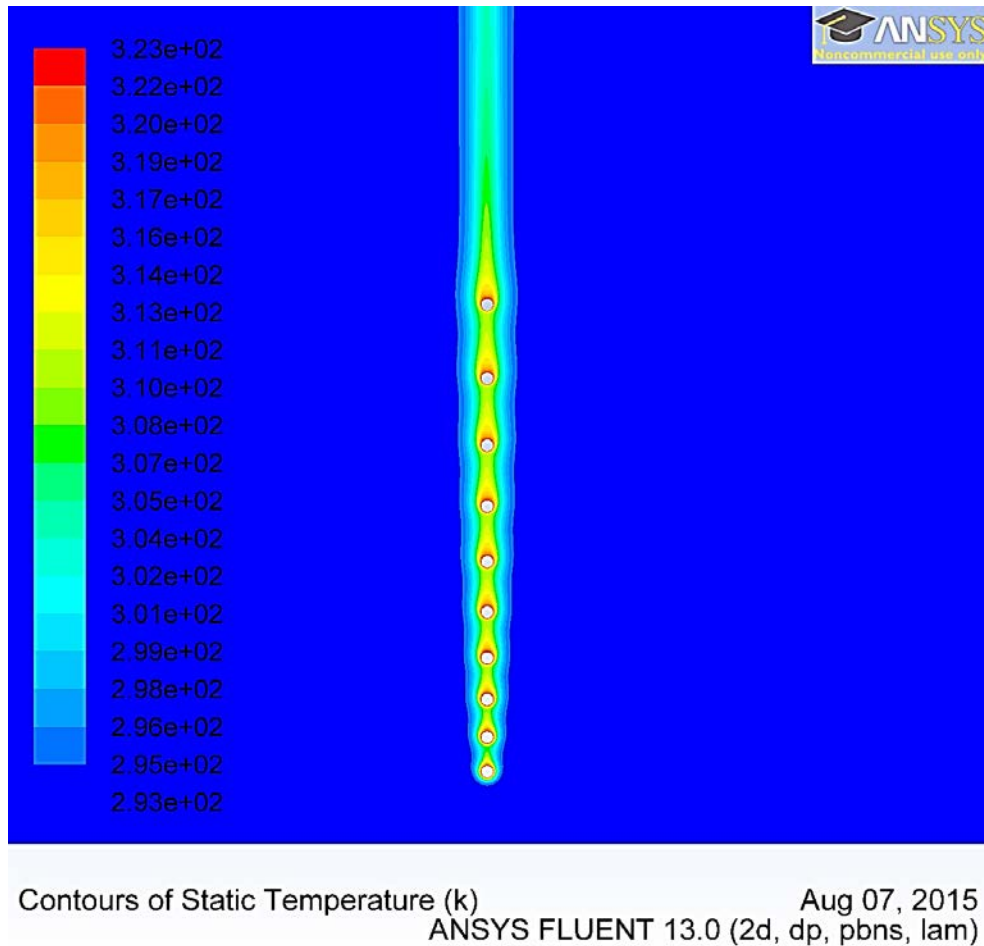


Figure 2.17 Cylinders in a vertical array with the aspect ratio $x=1.1$, $T_s=323$ K, $T_a=293$ K

CHAPTER 3

RESULTS AND DISCUSSION

The study presented in this paper was numerically studied in FLUENT package and it was found out that the distances between the vertically arranged horizontal cylinders have great influence on the heat transfer of each cylinder and the whole bundle of cylinders.

The first results shared below are those for the first distance S_1 (between 1st and 2nd cylinder) at 10 cylinder diameter. The graphs are those of the cases having 5 vertically arranged copper cylinders in air.

For the S_1 distances having less than $7D$, different outcomes in the vertical array in terms of heat transfer were found. These cases ($S_1=2D, 3D, 5D$) are also discussed in the following part.

Using the same spacing between the cylinders results in slightly decreased heat transfer occurring at the upper cylinders. In addition, the analysis utilizing the magnitude of aspect ratio (x) as 0.8, 0.9 and 0.95, which means decreasing spacing of the cylinders in the direction of upstream, showed a dramatic decrease in the heat transfer of the cylinders.

The results of the analysis have shown that the dissimilar spacing of the cylinders has a great impact on the heat transfer of each cylinder. As the aspect ratio (x) increases, the lower cylinder affects the upper cylinders less in terms of temperature which is the function of heat transfer. Such an increasing distance does not result in a great decrease of the heat transfer made from upper cylinders.

3.1 Results for the 5 Cylinder Cases

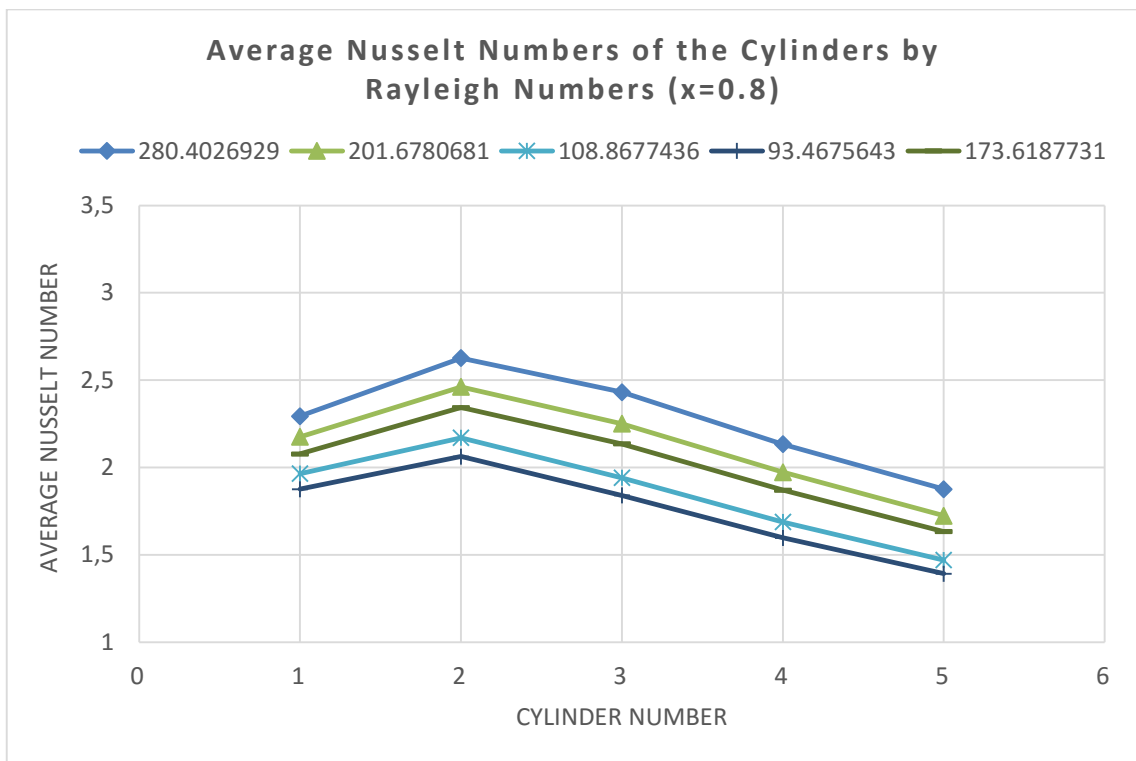


Figure 3.1 Aspect ratio, $x=0.8$, $S_1=10D$, 5 cylinder case, Nusselt number of each cylinder

When the aspect ratio equals 0.8, the separation distances of the cylinders are getting smaller upwards. As can be seen in Figure 3.1, the Nusselt number reached its peak point in the second cylinder, while a steady decline occurred after the second cylinder. Besides this, the Nusselt number of the fifth cylinder is corresponding to 75% of the first cylinder's Nusselt number.

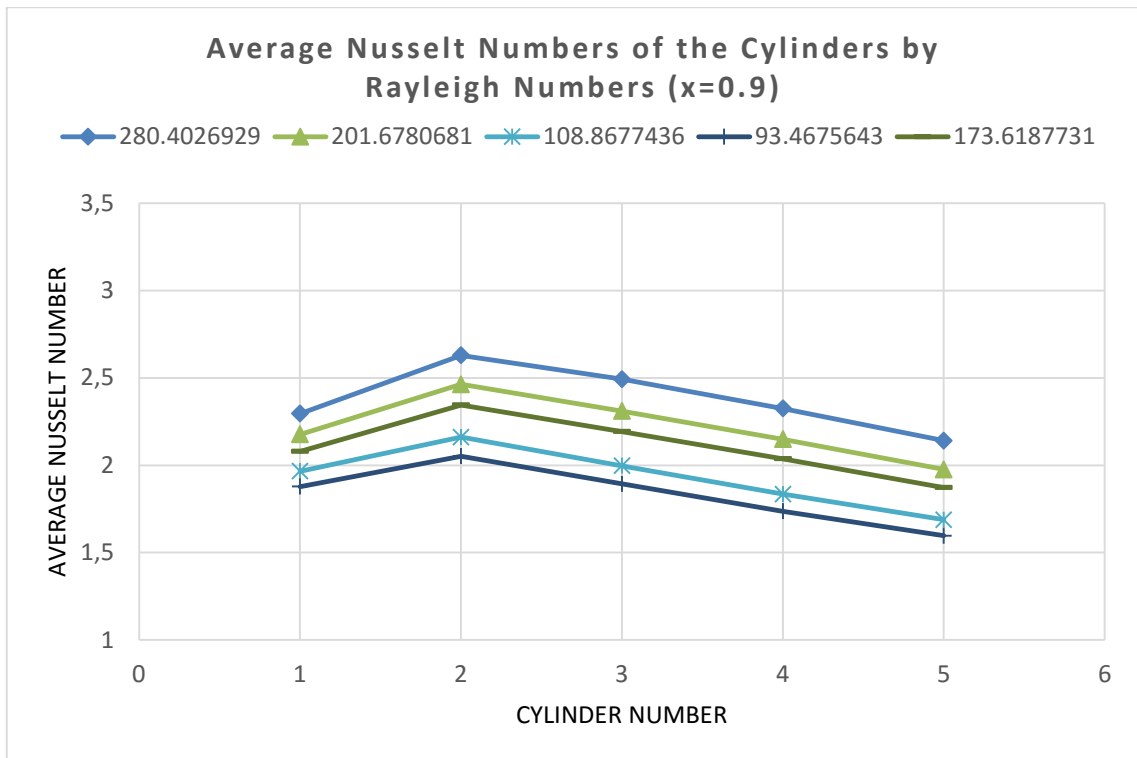


Figure 3.2 Aspect ratio $x=0.9$, $S_1=10D$, 5 cylinder case, Nusselt number of each cylinder

Changing the aspect ratio to 0.9 (Figure 3.2), the results are improved in terms of the Nusselt number. This slight improvement is visible from the 3rd cylinder on. While the Rayleigh number was around 280, the 5th cylinder's Nusselt number has risen from 1.87 to 2.14 as the aspect ratio changed from 0.8 to 0.9. This result is already a sign of the negative effect of the decreasing distances in the vertical array. Comparing Figure 3.1 and Figure 3.2 leads to anticipating the heat transfer improvement in the cases having the aspect ratio (x) as 0.95 and 1 (steady distance) which are shown below.

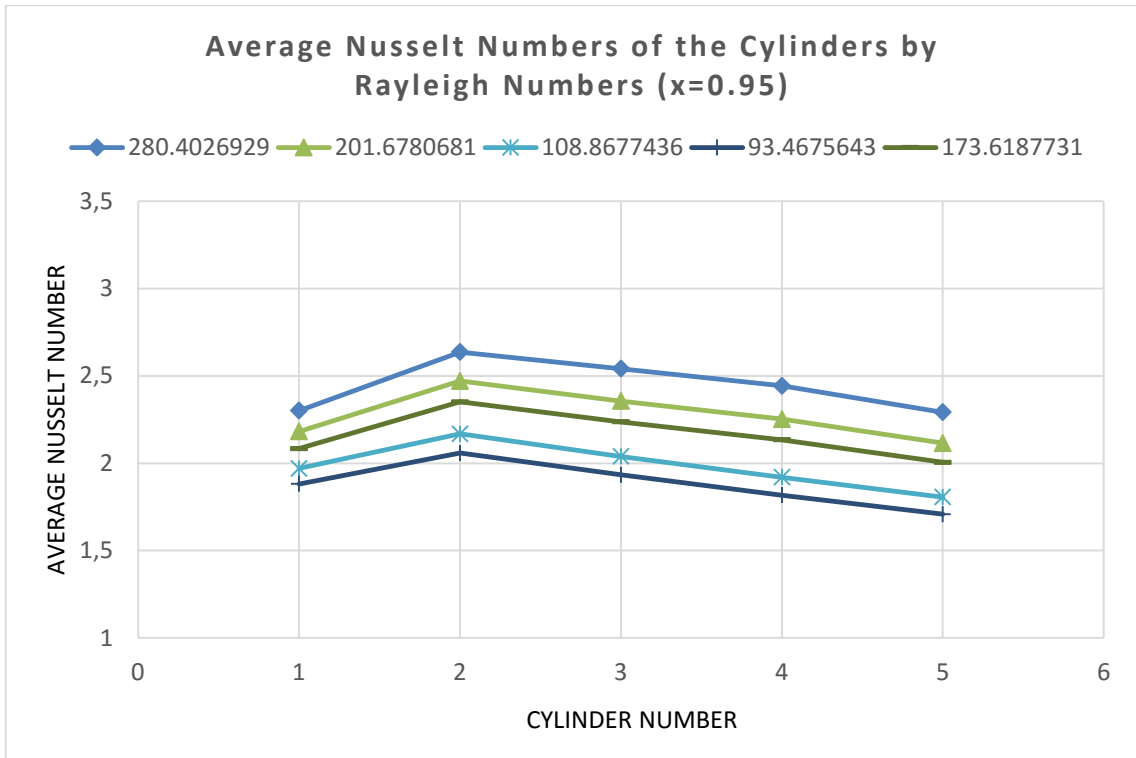


Figure 3.3 Aspect ratio $x=0.95$, $S_1=10D$, 5 cylinder case, Nusselt number of each cylinder

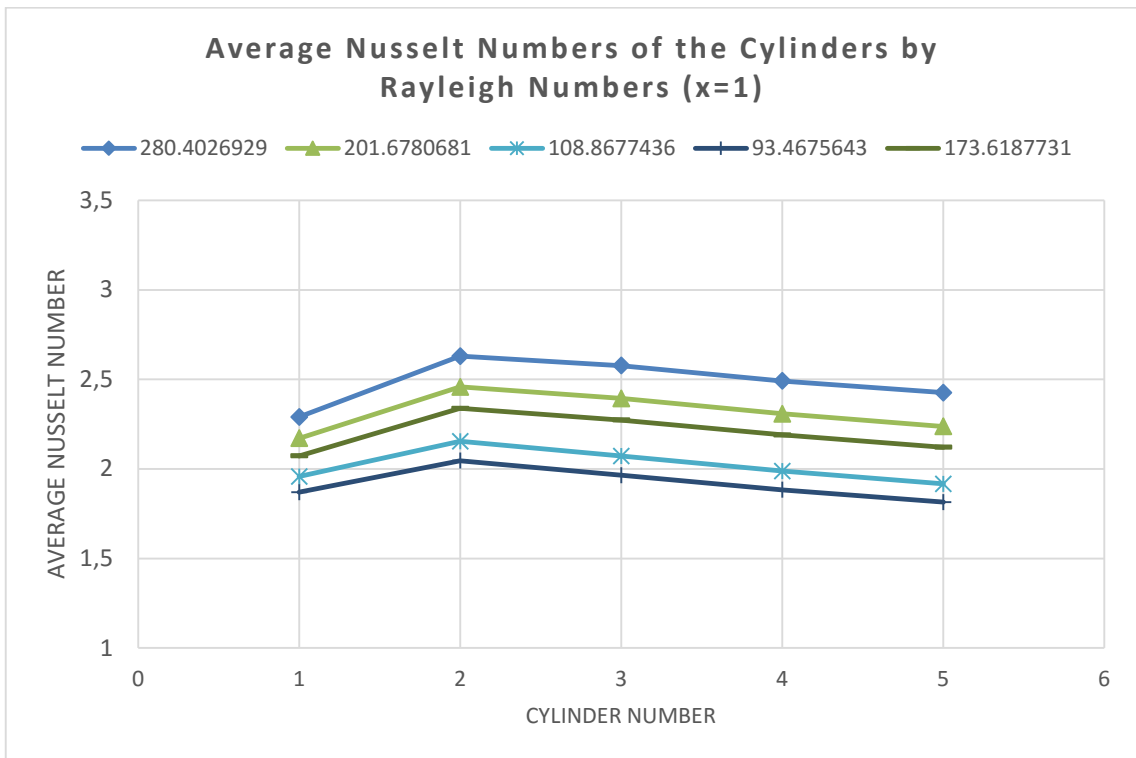


Figure 3.4 Aspect ratio $x=1$, $S_1=10D$, 5 cylinder case, Nusselt number of each cylinder
 Figure 3.4, in which the separation distances are constant between the 3rd, 4th and 5th cylinder, the cylinders' Nusselt numbers are slightly increased compared to the cases

with decreasing separation distances presented in Figures 3.1, 3.2, 3.3. The reason why the 1st and 2nd cylinders' Nusselt numbers do not change is the same distance of the cylinders of $S_1=10$ cylinder-diameter.

After the rise in the second cylinder, there is a clear decrease in the rest of the cylinders, as can be seen in Figures 3.1, 3.2, 3.3 and 3.4.

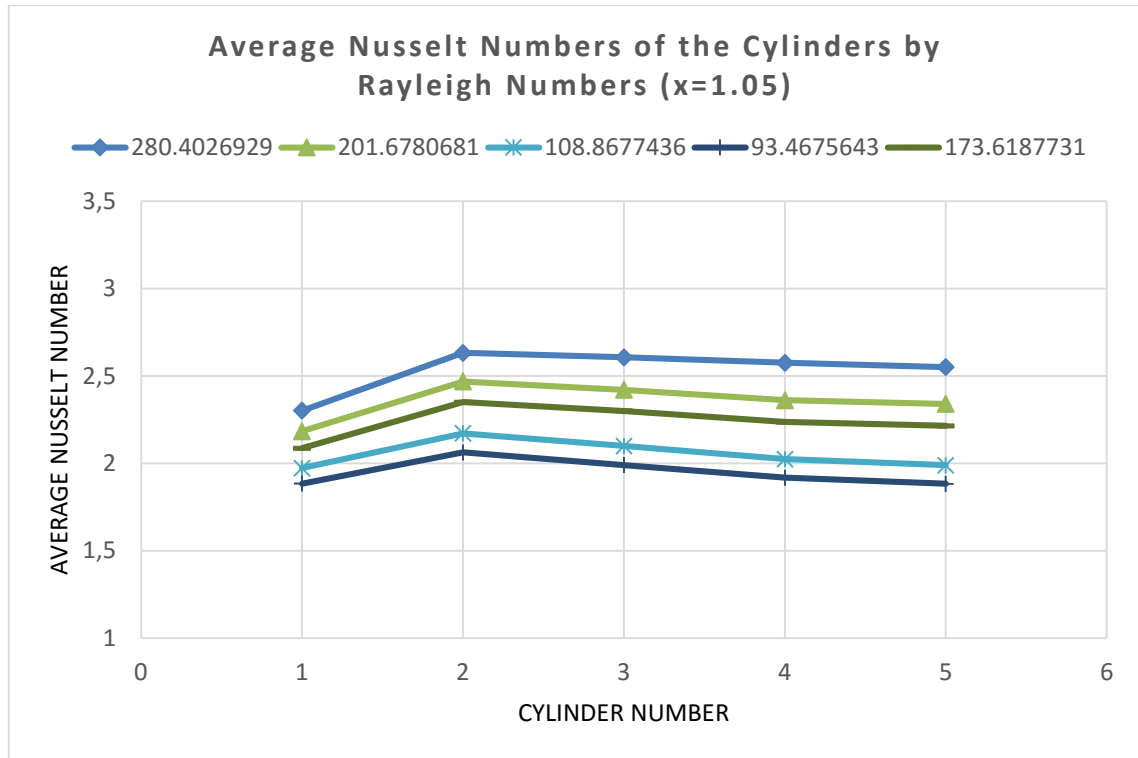


Figure 3.5 Aspect ratio $x=1.05$, $S_1=10D$, 5 cylinder case, Nusselt number of each cylinder

Regarding Figure 3.5, although the Nusselt numbers of the cylinders 3, 4 and 5 are lower than the 2nd cylinder's Nusselt number, their value is still higher than the 1st cylinder's. This clearly shows that using the aspect ratio of $x=1.05$ to increase the distance between the cylinders can diminish the heat transfer loss of the cylinders located after the 2nd cylinder.

Having the aspect ratio of $x=1.1$ (Figure 3.6), the Nusselt numbers of the cylinders located above the 2nd cylinder present horizontal lines in the graph.

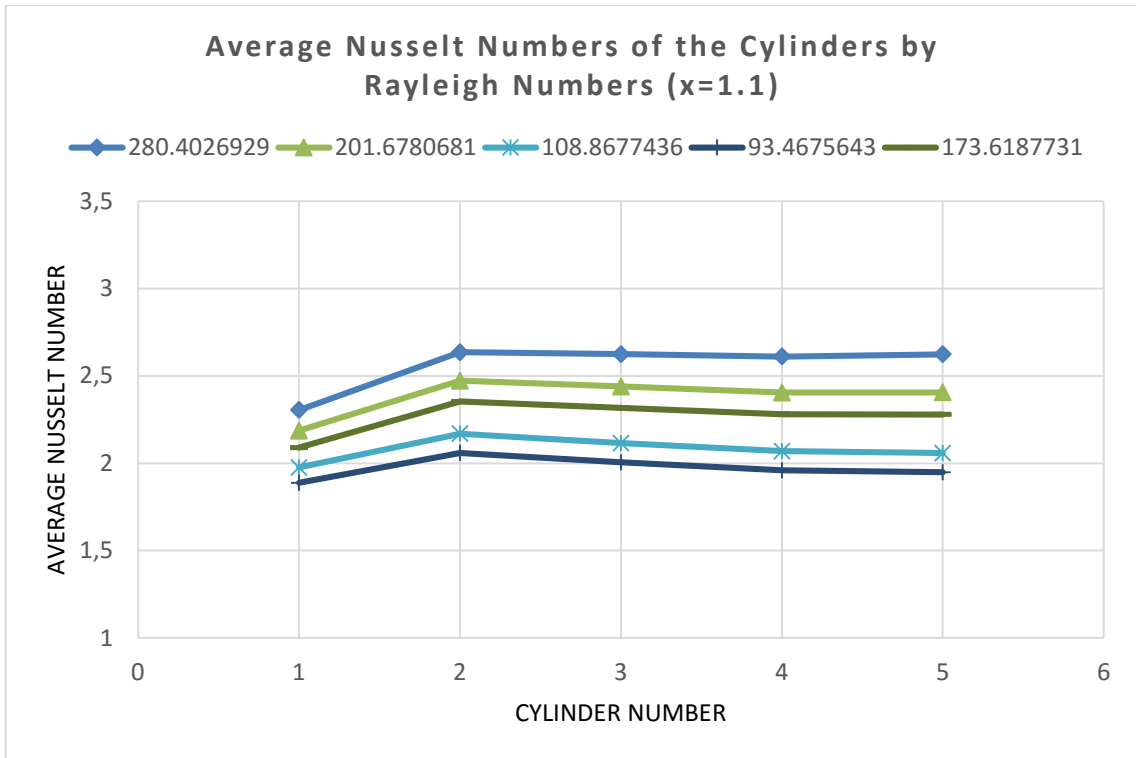


Figure 3.6 Aspect ratio $x=1.1$, $S_1=10D$, 5 cylinder case, Nusselt number of each cylinder

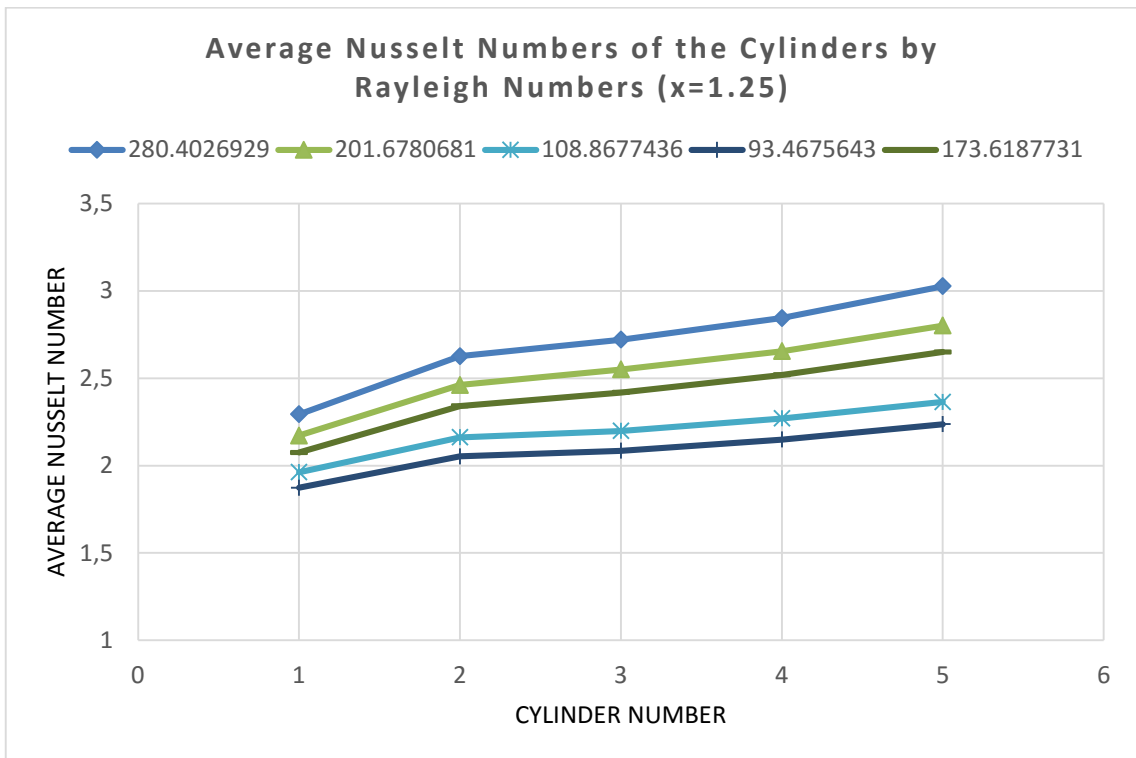


Figure 3.7 Aspect ratio $x=1.25$, $S_1=10D$, 5 cylinder case, Nusselt number of each cylinder

As the highest aspect ratio ($x=1.25$) was applied to the case, shown in Figure 3.7, the increasing distances in a longer range gave better Nusselt number results in the bundle.

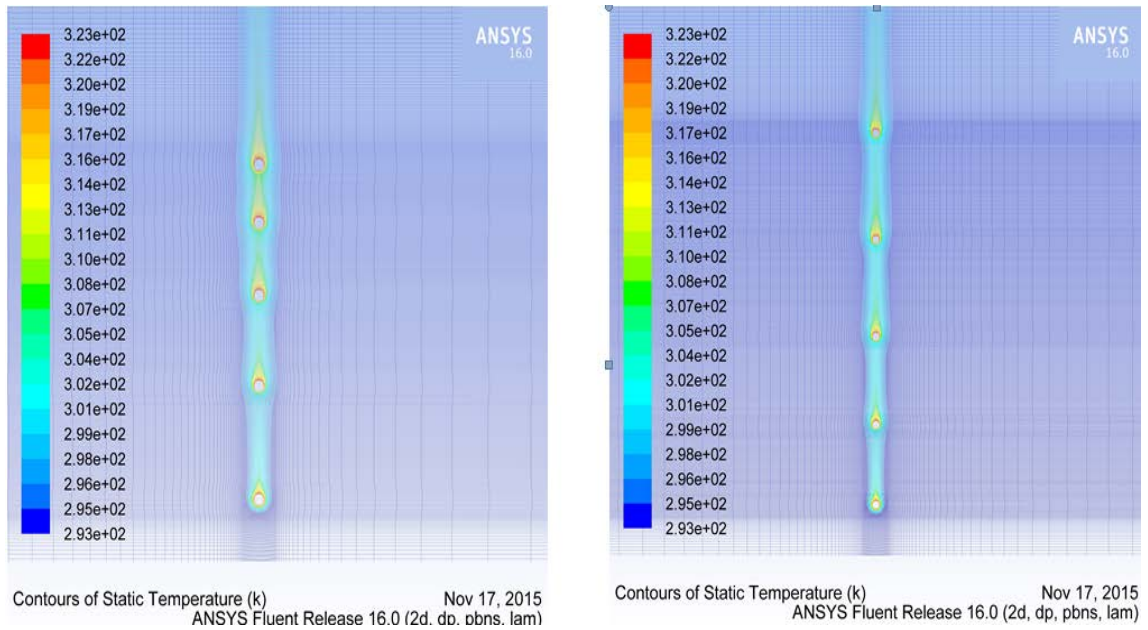


Figure 3.8 Aspect ratio $x=0.8$ (left) and $x=1.1$ (right)

As mentioned before, Grafton and Jensen [22] have studied decreasing distances and an enhancement in the 3rd cylinder in terms of the Nusselt number was found. However, the reason of these different results was having a comparatively higher Rayleigh number.

3.2 First Distance Effect on Heat Transfer

In this part of the results, for 3 different increasing aspect ratios and for 5 different S_1 separation distances, the Nusselt number of each cylinder is examined whilst the Rayleigh number is at 280. The first conspicuous outcome of these spacings is the Nusselt number of the second cylinder, showing a significant decrease up to 66% of the value of the first cylinder in the case of the first spacing as 2 cylinder diameter.

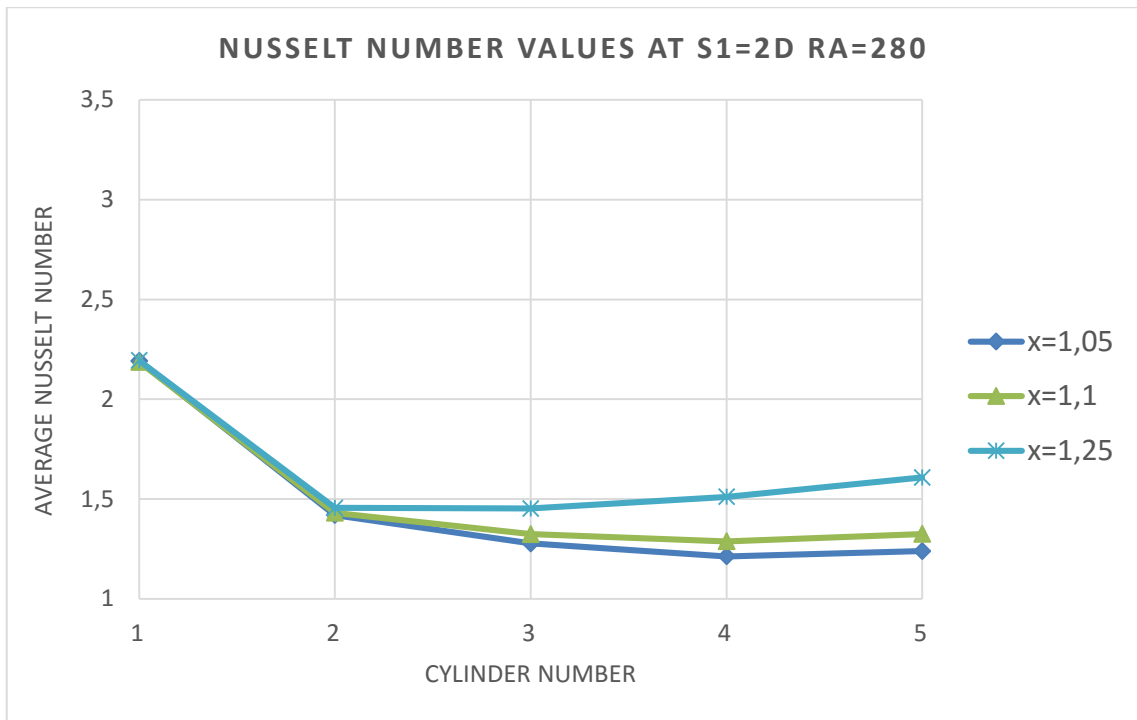


Figure 3.9 Nusselt numbers of 5 cylinders in a vertical array within $S_1=2D$

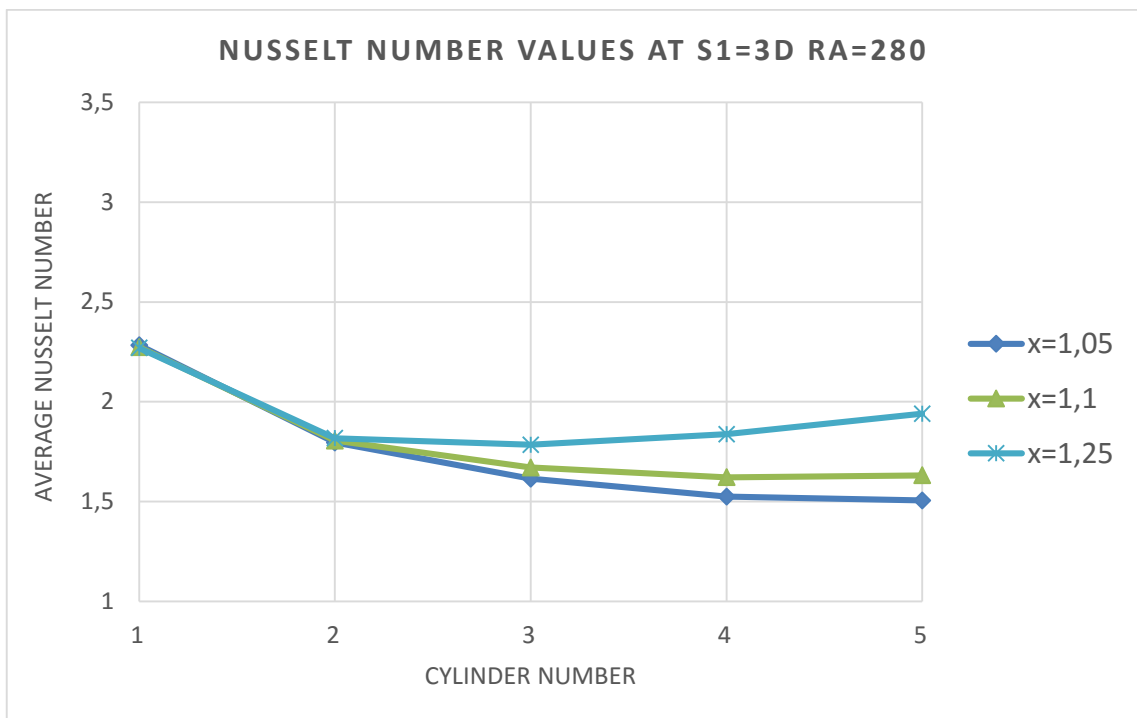


Figure 3.10 Nusselt numbers of 5 cylinders in a vertical array within $S_1=3D$

The drop in the Nusselt number of the second cylinder is less in the $S_1=3D$ case. The second cylinder has 77% of the first cylinder's Nusselt number. For the cylinders above the second cylinder, the Nusselt number graph shows a parallel line when being compared to the previous graph in which S_1 equals $2D$. In spite of the parallel line of the

graph when $S_1=3D$, the upper cylinders showed almost 20% improvement in terms of Nusselt number in comparison with the case of $S_1=2D$. Table 3.1 presents the total convection heat transfer rates for the bundle. It can be seen that the improvement in convection heat transfer rate is around 17% for the case of $x=1.25$ aspect ratio.

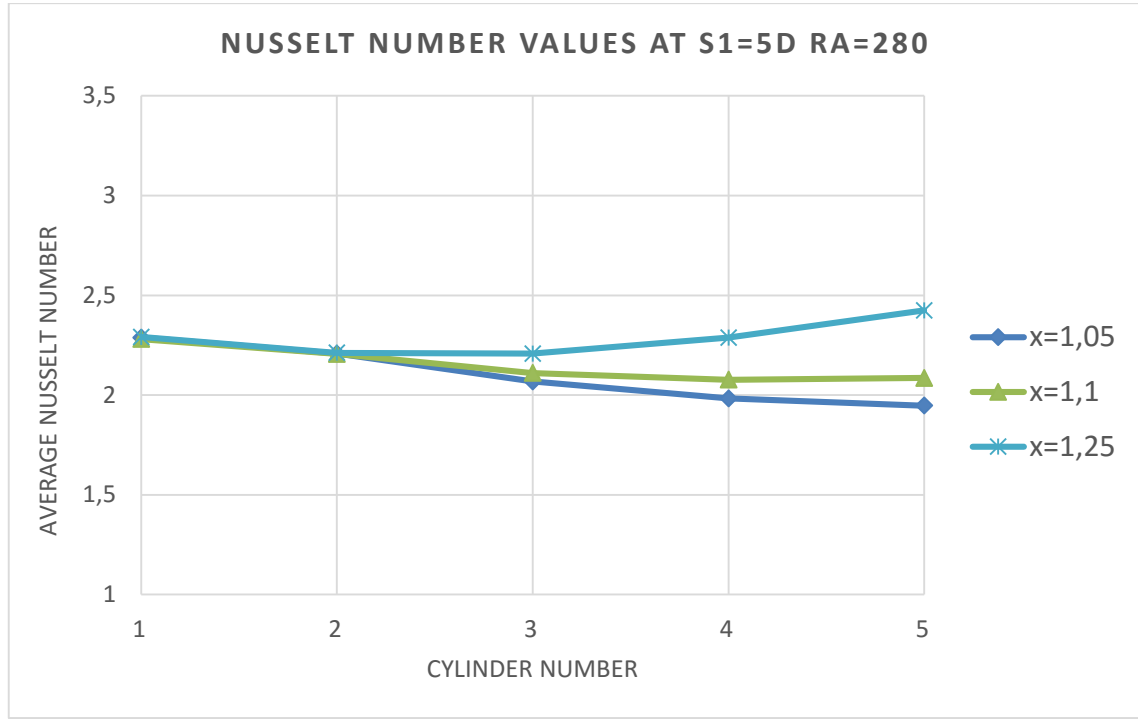


Figure 3.11 Nusselt numbers of 5 cylinders in a vertical array within $S_1=5D$

When the distance comes to 5 cylinder diameter, the temperature effect of the first cylinder on the second cylinder reduces dramatically. Therefore, the second cylinder's Nusselt number has shown a slight decrease of around 4% compared to the first cylinder. The cylinders located upper than the second cylinder differ from each other in terms of the Nusselt number, as the aspect ratio rises. Figure 3.11 shows that the Nusselt numbers of the 5th cylinder were higher than the lower cylinders' Nusselt number within the aspect ratio of 1.25.

In the light of the figures shared above, it can be stated that the second cylinder's behavior strongly depends on the spacing S_1 between the first and the second cylinder. Besides this, it can be anticipated that when S_1 increases, the second cylinder will show even higher rates of convection heat transfer. The graphs presenting the results of the cases having greater spacings are shown below.

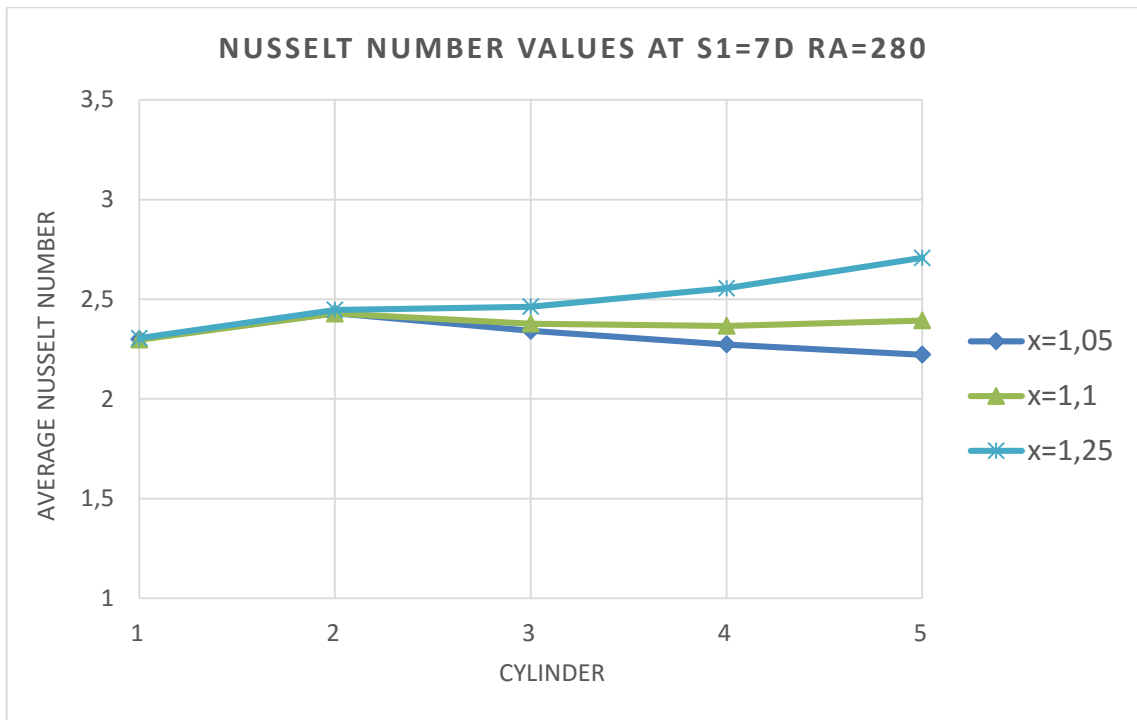


Figure 3.12 Nusselt numbers of 5 cylinders in a vertical array within $S_1=7D$

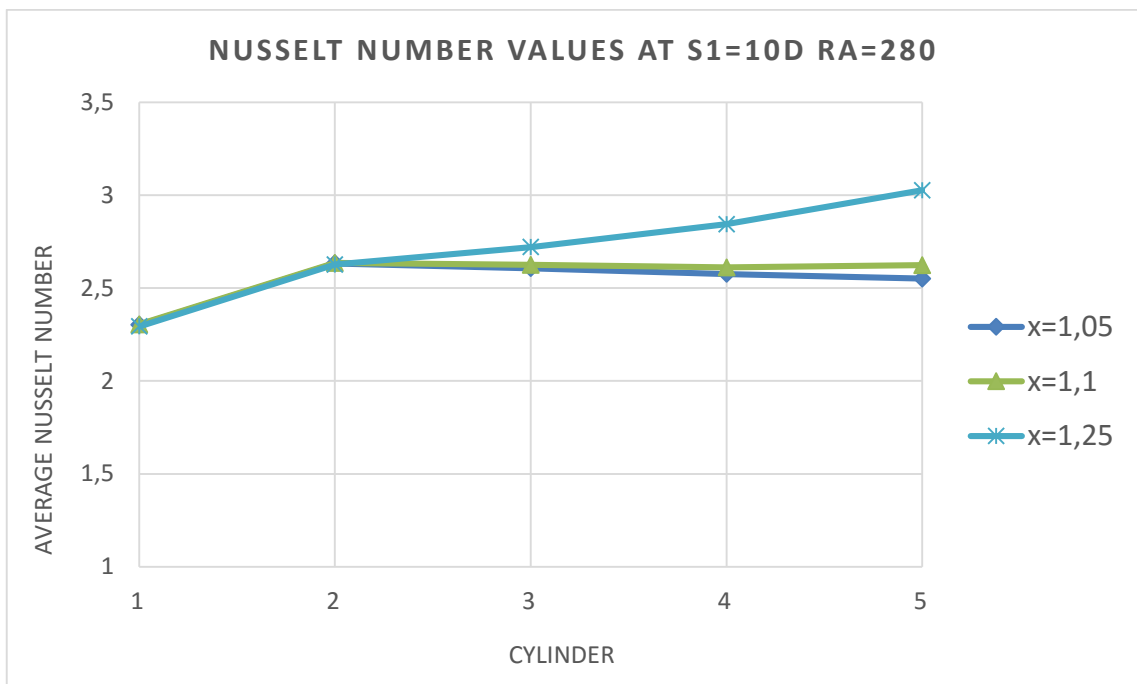


Figure 3.13 Nusselt numbers of 5 cylinders in a vertical array within $S_1=10D$

While a decrease has been seen on the second cylinder for the cases with $S_1=2D$, $3D$ and $5D$, an increase occurred in the cases having the separation distance as $S_1=7D$ and $10D$.

Another result worth to share is that the second cylinder slightly affected the first cylinder in the cases of 2D and 3D. While the Nusselt number of the first cylinder was 2.2 for the 2D separation distance, it was 2.3 for the 5D.

On the contrary, the study of the Reymond [6] claimed that for the distances larger than 1.5D, the first cylinder is unaffected by the upper cylinder. However, the present study showed that for the case having 2D separation distance, the first cylinder's Nusselt number decreased 4% compared to the larger spacings or one cylinder alone. This decrease was around 1% for the case of $S_1=3D$.

Good agreement with the study of Sadeghipour and Asheghi [11] is seen concerning the first and the second cylinder's interaction. The second cylinder's Nusselt number starts to be higher than the first cylinder's Nusselt number from the distance of 5D on. In contrast, comparing the present results with Corcione [5], shows a disagreement regarding the Nusselt number of the second cylinder. While Corcione found an enhancement for the 4D and larger spacings, the present study found an enhancement for 5D or larger spacings.

The results of the present study compared with the previous studies are shown in Figure 3.14 below.

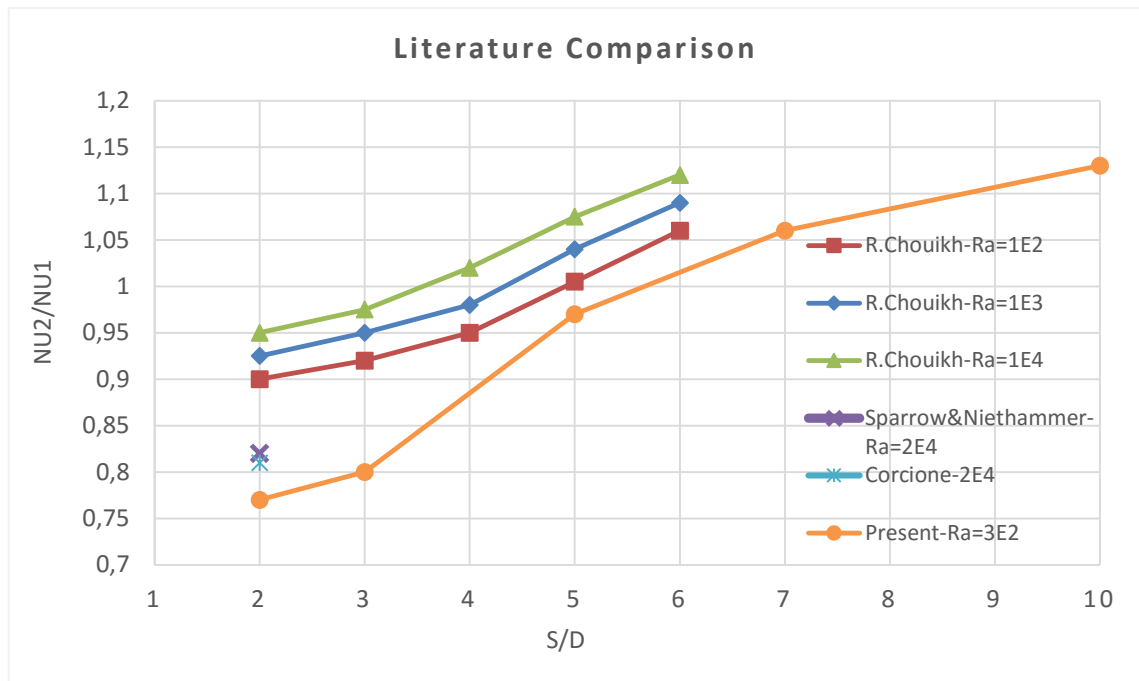


Figure 3.14 Literature comparison of the Nusselt numbers changing with S/D

The results of the numerical and experimental study of Chouikh et al. [13], [14] and the present study showed a parallel line. A good agreement for the larger S_1/D distances exists, but the ratios of the Nusselt numbers were not matching well.

3.3 Average Nusselt Number in the Bundle

The Nusselt numbers of the cylinders were investigated above. However, in this part of the study the average Nusselt number of the bundle was examined which gives the total amount of heat transfer.

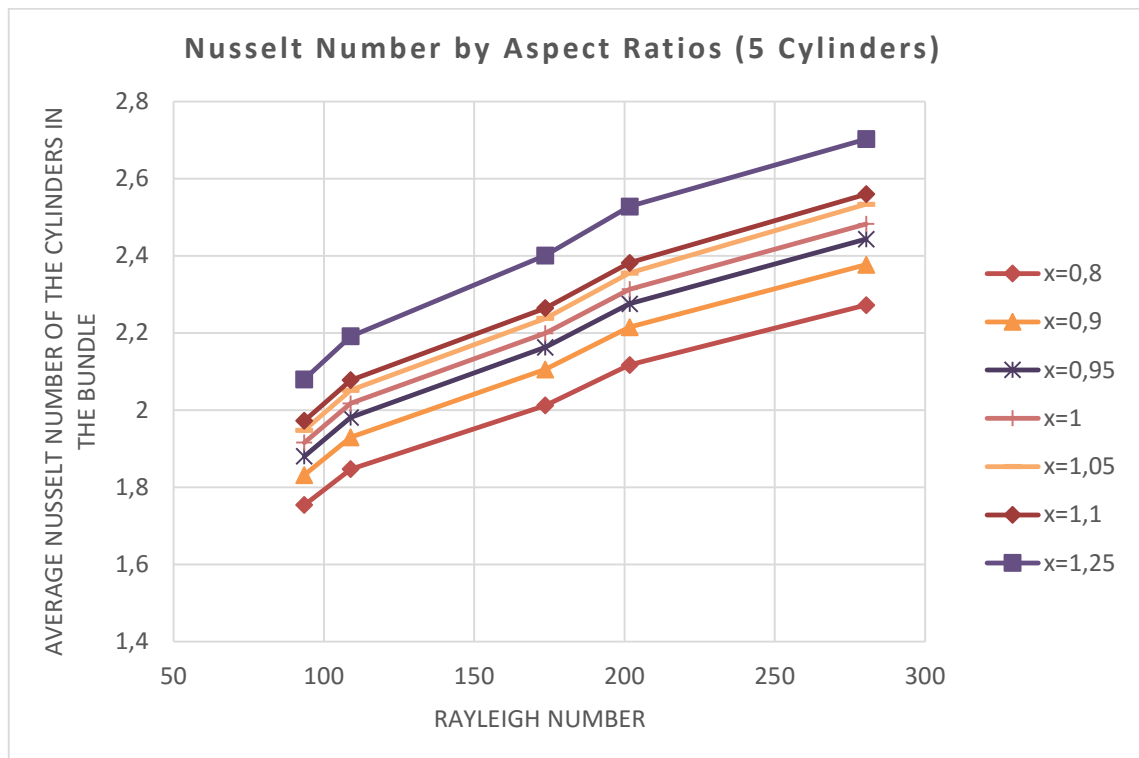


Figure 3.15 Average Nusselt numbers of the bundle in different aspect ratios

While the Rayleigh number equals 280, the surface of the cylinders is 323 K and the ambient temperature is 293 K. This temperature difference is the function of the Rayleigh number as can be seen from the equation (1.28). Figure 3.15 represents the average Nusselt numbers of the cylinders in the bundle for the cases of 7 different aspect ratios. As can be derived from the figure, the higher the aspect ratio's value, the higher is the Nusselt number in the bundle. For the highest Rayleigh number value, the difference of the Nusselt number is almost 0.5 between the aspect ratios of 0.8 and 1.25.

The results found in this study in terms of the convection heat transfer and the total heat transfer rates are shown in the tables below. One can easily see an increase in the total heat transfer rates when a case has higher S_1 and higher aspect ratio values.

Table 3.1 Convection heat transfer rates

Convection Heat Transfer Rate (W)							
aspect ratio (x)	2 pipes	3 pipes	4 pipes	5 pipes	7 pipes	10 pipes	S ₁ /D
1						29.39	2
1.05	9.10	12.24	15.20	18.16	23.77	32.12	2
1.1	9.10	12.37	15.55	18.69	25.15	34.90	2
1.25	9.10	12.67	16.39	20.34	29.26	45.35	2
1						36.67	3
1.05	10.09	14.13	17.74	21.54	28.75	39.14	3
1.1	10.09	14.20	18.03	22.27	30.45	42.53	3
1.25	10.09	14.52	19.11	23.87	34.31	53.14	3
1						45.00	5
1.05	11.08	16.17	21.05	25.96	35.63	49.51	5
1.1	11.08	16.32	21.45	26.62	36.34	51.73	5
1.25	11.08	16.57	22.00	28.26	41.48	61.48	5
1						52.93	7
1.05	11.64	17.46	23.08	28.63	39.49	55.00	7
1.1	11.64	17.54	23.40	29.35	40.78	57.29	7
1.25	11.64	17.79	24.17	30.87	46.14	68.77	7
1						58.29	10
1.05	12.13	18.63	25.06	31.34	42.97	59.40	10
1.1	12.13	18.74	25.41	31.67	44.86	65.89	10
1.25	12.13	18.92	26.06	33.43	50.38	72.99	10

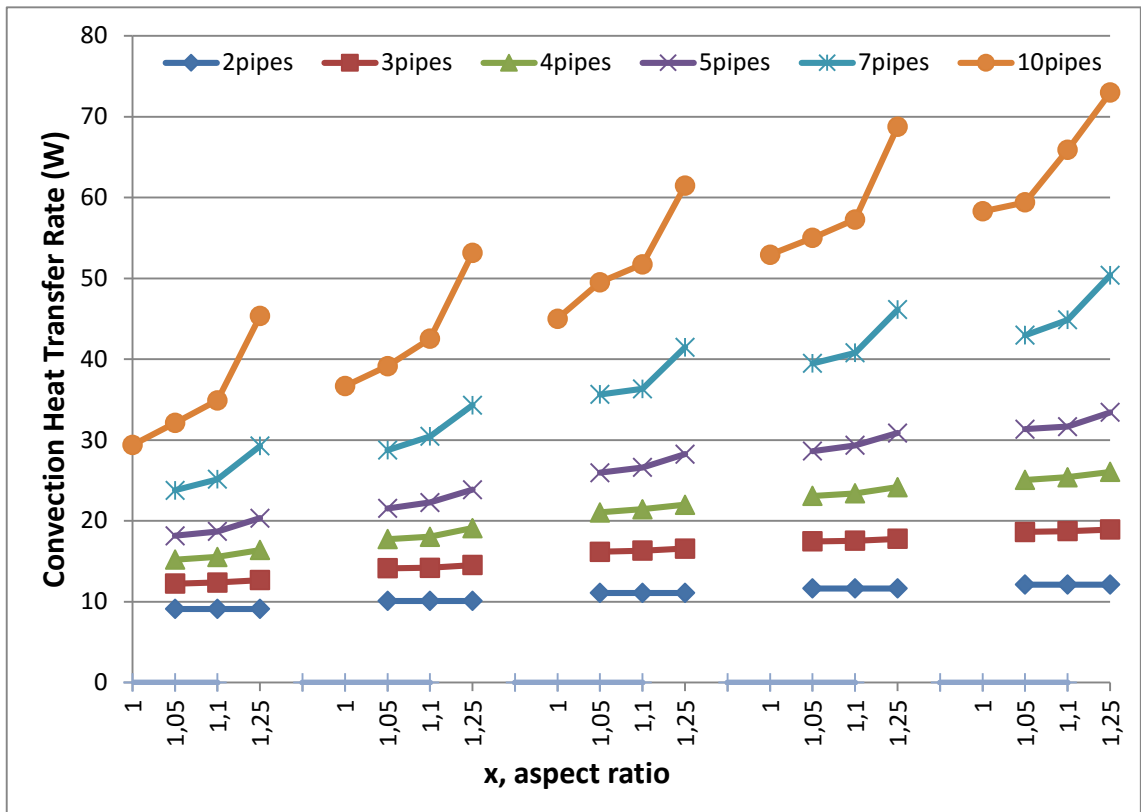


Figure 3.16 Total convection heat transfer rate for each S₁/D case

Table 3.2 Total heat transfer rate for each case

Total Heat Transfer Rate (W)							
aspect ratio (x)	2 pipes	3 pipes	4 pipes	5 pipes	7 pipes	10 pipes	S ₁ /D
1						43.12	2
1.05	11.96	16.47	20.81	25.14	33.54	46.10	2
1.1	11.96	16.61	21.17	25.71	35.00	49.04	2
1.25	11.96	16.93	22.07	27.45	39.27	59.76	2
1						50.87	3
1.05	13.00	18.47	23.50	28.72	38.79	53.48	3
1.1	13.00	18.53	23.80	29.47	40.53	56.98	3
1.25	13.00	18.87	24.91	31.12	44.50	67.76	3
1						59.53	5
1.05	14.03	20.58	26.91	33.27	45.86	64.12	5
1.1	14.03	20.72	27.32	33.95	46.59	66.40	5
1.25	14.03	20.98	27.88	35.61	51.79	76.25	5
1						67.60	7
1.05	14.61	21.89	28.99	35.99	49.79	69.72	7
1.1	14.61	21.97	29.30	36.73	51.12	72.05	7
1.25	14.61	22.23	30.08	38.22	56.51	83.60	7
1						73.06	10
1.05	15.10	23.09	30.99	38.75	53.33	74.21	10
1.1	15.10	23.19	31.34	39.08	55.23	80.72	10
1.25	15.10	23.38	32.00	40.85	60.79	87.87	10

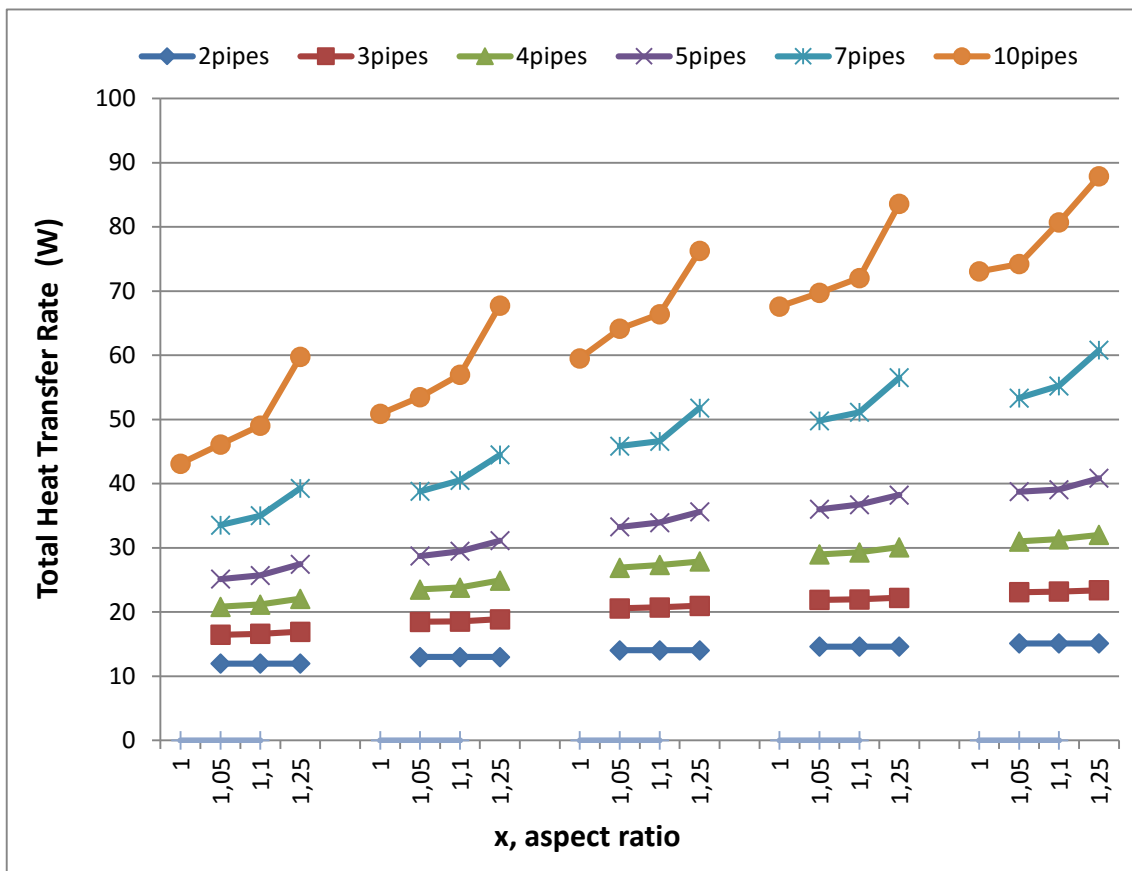


Figure 3.17 Total heat transfer rate for 5 different S₁/D values

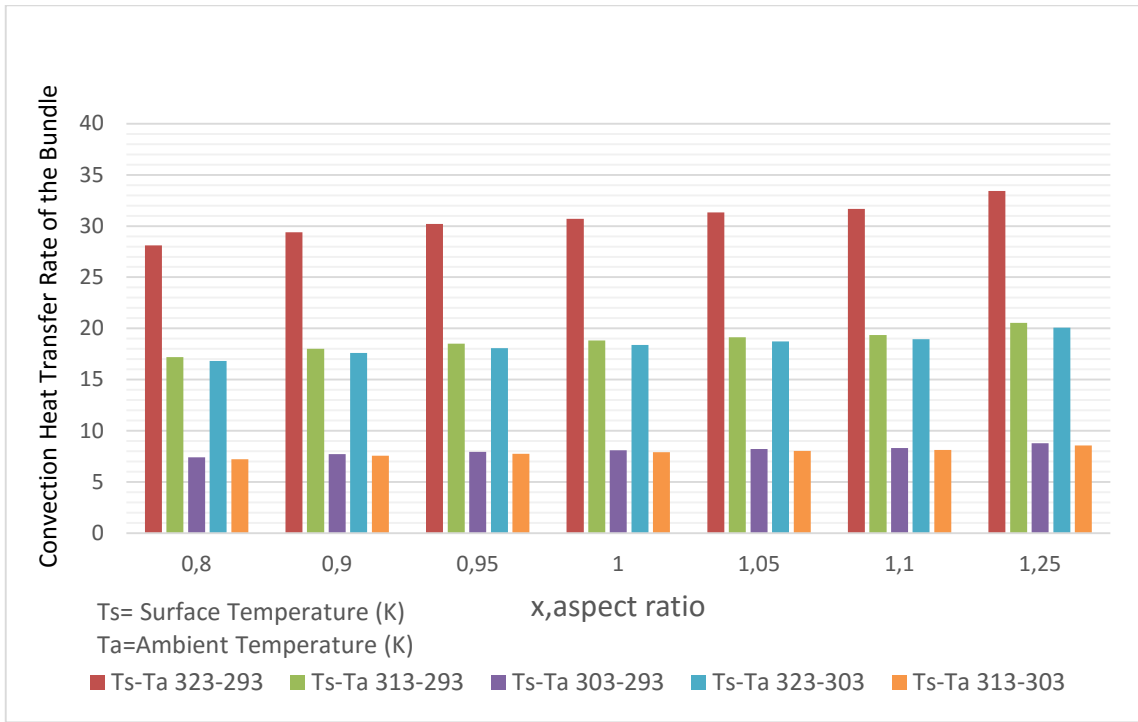


Figure 3.18 Convection heat transfer rates of 5 cylinder cases

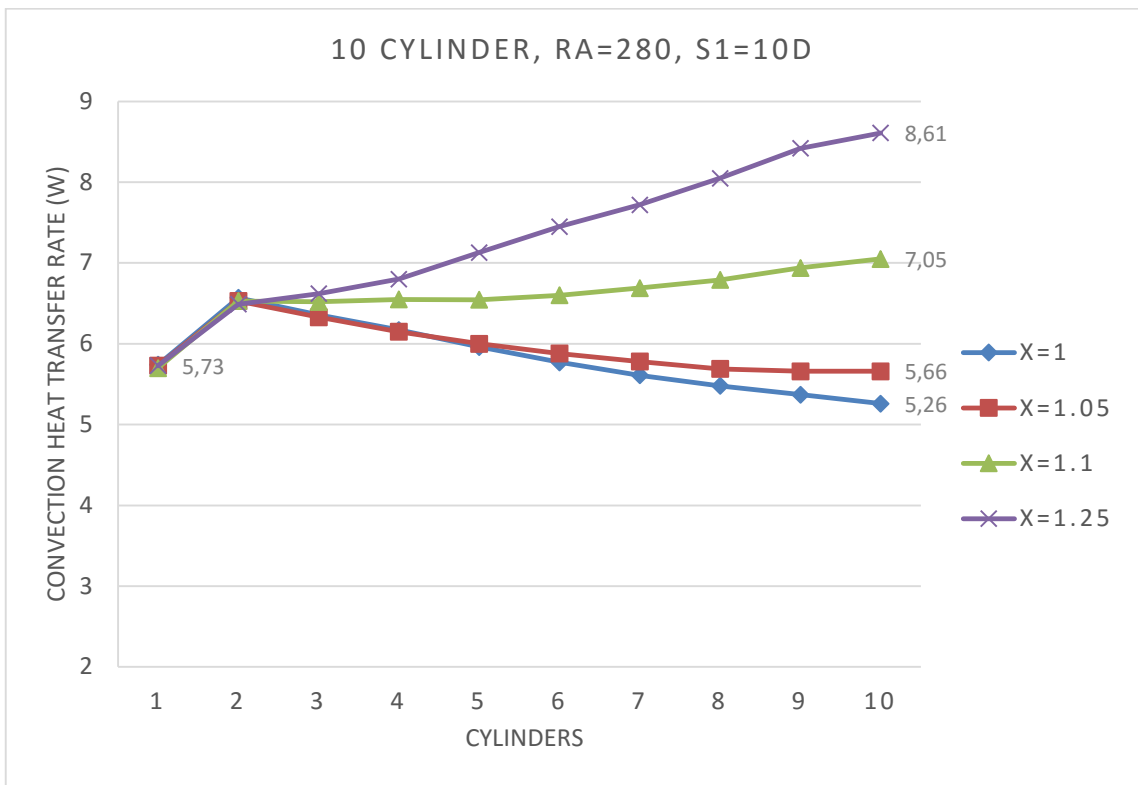


Figure 3.19 Convection heat transfer rates of all 10 cylinders

3.4 Summary

The effect of dissimilar spacing of vertically aligned horizontal cylinders has been investigated. The results can be summarized as following,

- For each different Rayleigh number (93, 108, 173, 201 and 280) and the S_1 value of 7D and 10D, the Nusselt number of the second cylinders increased up to 6% and 13% respectively, while it decreased in the cases of $S_1 = 2D$, 3D and 5D with rates of 33%, 20% and 3% respectively.
- In the cases having $S_1 = 7D$ and 10D and different aspect ratios ranging from 0.8 to 1.25, the Nusselt number of the second cylinder showed a significant rise.
- For all five different Rayleigh numbers, the average Nusselt number of the bundle increased when the aspect ratio increased.

For the cases of $S_1 = 10D$ and 5 cylinders;

- When the aspect ratio equaled (x) = 0.8, 0.9, 0.95, 1 and 1.05, a rise of the Nusselt number was seen in the second cylinder, but the 3rd, 4th and 5th cylinder showed a decrease of the Nusselt number.
- Within the aspect ratio of $x = 1.1$, the reduction disappeared and the upper cylinders showed a stable magnitude of Nusselt number.
- For $x = 1.25$, the Nusselt numbers of the upper cylinders increased constantly.

The plume rising from the lower cylinder had a negative effect on the upper cylinders in terms of temperature.

Using increasing distances,

- The temperature effect diminished and the buoyancy force increased with the increasing velocity upwards. This resulted in an increase of the heat transfer.
- Increasing distance provides a higher heat transfer rate so less cylinders can be used to achieve the same heat transfer rate for the bundle.

REFERENCES

- [1] Tillman, E.S., (1976). “Natural Convection Heat Transfer from Horizontal Tube Bundles”, ASME, 76-HT-35.
- [2] Farouk, B. and Guceri S., (1983). “Natural Convection from Horizontal Cylinders in Interacting Flow Fields”, *Int. J. Heat Mass Transfer*, 26: 231–243.
- [3] Farouk, B. and Guceri, S., (1981). “Natural Convection from a Horizontal Cylinder, Laminar Regime”, *Journal of Heat Transfer*, 103(3): 522–527.
- [4] Corcione, M., (2005). “Correlating Equations for Free Convection Heat Transfer from Horizontal Isothermal Cylinders Set in a Vertical Array”, *Int. J. Heat Mass Transfer*, 48: 3660–3763.
- [5] Corcione, M., (2007). “Interactive Free Convection from a Pair of Vertical Tube-Arrays at Moderate Rayleigh Numbers”, *Int. J. Heat Mass Transfer*, 50: 1061–1074.
- [6] Reymond, O., Murray, D.B. and O'Donovan, T.S., (2008). “Natural Convection Heat Transfer from Two Horizontal Cylinders”, *Experimental Thermal and Fluid Science*, 32: 1702–1709.
- [7] Lieberman, J. and Gebhart, B., (1969). “Interaction in Natural Convection from an Array of Heated Elements, Experimental”, *Int. J. Heat Mass Transfer*, 12: 1385–1396.
- [8] Marsters, G.F., (1972). “Arrays of Heated Horizontal Cylinders in Natural Convection”, *Int. J. Heat Mass Trans.*, 15: 921–933.
- [9] Sparrow, E.M. and Niethammer, J.E., (1981). “Effect of Vertical Separation Distance and Cylinder-to-Cylinder Temperature Imbalance on Natural Convection for a Pair of Horizontal Cylinders”, *J. Heat Transfer*, 103: 638-644.
- [10] Tokura, I., Saito, H., Kishinami, K. and Muramoto, K., (1983). “An Experimental Study of Free Convection Heat Transfer from a Horizontal Cylinder in a Vertical Array Set in Free Space between Parallel Walls”, *Transactions of the ASME*, 105: 102 – 107.
- [11] Sadeghipour, M.S. and Asheghi, M., (1994). “Free Convection Heat Transfer from Arrays of Vertically Separated Horizontal Cylinders at Low Rayleigh Numbers”, *Int. J. Heat Mass Transfer*, 37 (1): 103–109.
- [12] Bejan, A., Fowler, A.J. and Stanescu, G., (1995). “The Optimal Spacing between Horizontal Cylinders in a Fixed Volume Cooled by Natural Convection”, *Int. J. Heat Mass Trans.*, 38 (11): 2047–2055.

- [13] Chouikh, R., Guizani, A., Maalej, M. and Belghith, A., (1999). “Numerical Study of the Laminar Natural Convection Flow around an Array of Two Horizontal Isothermal Cylinders”, *Int. Comm. Heat Mass Transfer*, 26: 329-338.
- [14] Chouikh, R., Guizani, A., El Cafsi, A., Maalej, M. and Belghith, A., (2000). “Experimental Study of The Natural Convection Flow Around an Array of Heated Horizontal Cylinders”, *Renew. Energy*, 21: 65–78.
- [15] Persoons, T., O’Gorman, I.M., Donoghue, D.B., Byrne, G. and Murray, D.B., (2011). “Natural Convection Heat Transfer and Fluid Dynamics for a Pair of Vertically Aligned Isothermal Horizontal Cylinders”, *Int. J. Heat Mass Trans.*, 54: 5163–5172.
- [16] D’Orazio, A. and Fontana, L., (2010). “Experimental Study of Free Convection from a Pair of Vertical Arrays of Horizontal Cylinders at Very Low Rayleigh Numbers”, *Int. J. Heat Mass Transfer*, 53: 3131–3142.
- [17] Yuncu, H. and Batta, A., (1994). “Effect of Vertical Separation Distance on Laminar Natural Convective Heat Transfer Over Two Vertically Spaced Equal Temperature Horizontal Cylinders”, *Appl. Sci. Res.*, 52: 259-277.
- [18] Sparrow, E.M. and Niethammer, J.E., (1981). “Effect of Vertical Separation Distance and Cylinder-to-Cylinder Temperature Imbalance on Natural Convection for a Pair of Horizontal Cylinders”, *J. Heat Transfer*, 103: 638-644.
- [19] Grafsonningen, S. and Jensen, A., (2012). “Natural Convection Heat Transfer from Two Horizontal Cylinders at High Rayleigh Numbers”, *International Journal of Heat and Mass Transfer*, 55: 5552–5564.
- [20] Kazemzadeh, S., Hannani, Sadeghipour, M.S., and Nazaktabar M., (2002). “Natural Convection Heat Transfer from Horizontal Cylinders in Vertical Array Confined Between Parallel Walls”, 15, 3: 293-301.
- [21] Stafford, J. and Egan, V., (2014). “Configurations for Single-Scale Cylinder Pairs in Natural Convection *International Journal of Thermal Sciences*, 84: 62-74.
- [22] Grafsonningen, S. and Jensen, A., (2013). “Natural Convection Heat Transfer from Three Vertically Arranged Cylinders with Dissimilar Separation Distance at Moderately High Rayleigh Numbers”, *International Journal of Heat and Mass Transfer*, 57: 519–527.
- [23] O’Gorman, I.M., Murray, D.B., Byrne, G. and Persoons, T., (2009). “Natural Convection from Isothermal Horizontal Cylinders”, *Proc. ASME Int. Mech. Eng. Congr., Florida, IMECE 2009*: 112-130.
- [24] Cengel, Y., (2002). “*Heat Transfer a Practical Approach*”, Second Edition, McGraw Hill, New York.
- [25] Bejan, A., (2013). “*Convection Heat Transfer*”, Forth Edition, John Wiley & Sons, Inc., New York.
- [26] Churchill, S.W. and Chu, H.H.S., (1975). “Correlating Equations for Laminar and Turbulent Free Convection from a Horizontal Cylinder”, *Int. J. Heat Mass Transfer*, 18: 1049–1053.

- [27] ANSYS FLUENT User's Guide,
<http://aerojet.engr.ucdavis.edu/fluenthelp/html/ug/node992.htm> ,
4th March 2016.
- [28] Fitzpatrick, R., 10th December 2015. "Teaching Fluid Mechanics", The
University of Texas at Austin
<http://farside.ph.utexas.edu/teaching/336L/Fluidhtml/node90.html> ,
8th March 2016.

APPENDIX-A

HEAT TRANSFER RATES

Table A.1 Radiation heat transfer rates for the cases

Radiation Heat Transfer Rate (W)							
aspect ratio (x)	2 pipes	3 pipes	4 pipes	5 pipes	7 pipes	10 pipes	S ₁ /D
1						13.73	2
1.05	2.86	4.23	5.61	6.99	9.77	13.98	2
1.1	2.86	4.24	5.63	7.03	9.85	14.14	2
1.25	2.86	4.26	5.67	7.11	10.01	14.41	2
1						14.20	3
1.05	2.91	4.33	5.76	7.18	10.04	14.34	3
1.1	2.91	4.34	5.77	7.20	10.08	14.45	3
1.25	2.91	4.35	5.80	7.25	10.19	14.62	3
1						14.52	5
1.05	2.95	4.40	5.86	7.31	10.23	14.61	5
1.1	2.95	4.41	5.87	7.33	10.26	14.67	5
1.25	2.95	4.41	5.88	7.35	10.31	14.77	5
1						14.67	7
1.05	2.97	4.43	5.90	7.37	10.30	14.72	7
1.1	2.97	4.43	5.91	7.38	10.33	14.76	7
1.25	2.97	4.44	5.91	7.35	10.37	14.83	7
1						14.77	10
1.05	2.98	4.45	5.93	7.41	10.36	14.80	10
1.1	2.98	4.45	5.94	7.42	10.37	14.83	10
1.25	2.98	4.46	5.94	7.42	10.40	14.88	10

Table A.2 Length of the vertical array

Total Length from the First Cylinder's Bottom to the Top of the Top Cylinder (mm)							
aspect ratio (x)	2 pipes	3 pipes	4 pipes	5 pipes	7 pipes	10 pipes	S ₁ /D
0,8	14,4	22,08	28,22	33,14	42,73	46,36	2
0,9	14,4	23,04	30,82	37,81	54,88	63,61	2
0,95	14,4	23,52	32,18	40,41	62,72	75,79	2
1	14,4	24,00	33,60	43,20	72,00	91,20	2
1,05	14,4	24,48	35,06	46,18	82,96	110,66	2
1,1	14,4	24,96	36,58	49,35	95,88	135,16	2
1,25	14,4	26,40	41,40	60,15	149,51	252,50	2
0,8	19,2	30,72	39,94	47,31	61,70	67,14	3
0,9	19,2	32,16	43,82	54,32	79,93	93,01	3
0,95	19,2	32,88	45,88	58,22	91,68	111,29	3
1	19,2	33,60	48,00	62,40	105,60	134,40	3
1,05	19,2	34,32	50,20	66,87	122,04	163,58	3
1,1	19,2	35,04	52,46	71,63	141,42	200,34	3
1,25	19,2	37,20	59,70	87,83	221,86	376,35	3
0,8	28,8	48,00	63,36	75,65	99,63	108,69	5
0,9	28,8	50,40	69,84	87,34	130,01	151,82	5
0,95	28,8	51,60	73,26	93,84	149,60	182,28	5
1	28,8	52,80	76,80	100,80	172,80	220,80	5
1,05	28,8	54,00	80,46	108,24	200,21	269,44	5
1,1	28,8	55,20	84,24	116,18	232,49	330,71	5
1,25	28,8	58,80	96,30	143,18	366,56	624,06	5
0,8	38,4	65,28	86,78	103,99	137,57	150,25	7
0,9	38,4	68,64	95,86	120,35	180,09	210,63	7
0,95	38,4	70,32	100,64	129,45	207,52	253,27	7
1	38,4	72,00	105,60	139,20	240,00	307,20	7
1,05	38,4	73,68	110,72	149,62	278,37	375,29	7
1,1	38,4	75,36	116,02	160,74	323,57	461,07	7
1,25	38,4	80,40	132,90	198,53	511,27	871,76	7
0,8	52,8	91,20	121,92	146,50	194,47	212,59	10
0,9	52,8	96,00	134,88	169,87	255,22	298,84	10
0,95	52,8	98,40	141,72	182,87	294,40	359,76	10
1	52,8	100,80	148,80	196,80	340,80	436,80	10
1,05	52,8	103,20	156,12	211,69	395,62	534,08	10
1,1	52,8	105,60	163,68	227,57	460,18	656,61	10
1,25	52,8	112,80	187,80	281,55	728,33	1243,31	10

CURRICULUM VITAE

PERSONAL INFORMATION

Name Surname : Sabri KALAY
Date of birth and place : 31.12.1989, Bafra/SAMSUN
Foreign Languages : English, German
E-mail : sabri.kalay.522@std.yildiz.edu.tr
sabrikalay@hotmail.com

EDUCATION

Degree	Department	University	Date of Graduation
Master	Mechanical Eng.	Yıldız Technical University	-
Undergraduate	Mechanical Eng.	Yıldız Technical University	2013
High School		Samsun Science High School	2008

PUBLISHERMENTS

Conference Papers

1. Kalay S., Demir H., Atayılmaz Ş.Ö., (2015). “Natural Convection Heat Transfer from Vertically Arranged Horizontal Cylinders”, International Conference on Energy Systems, 23-25 December 2015, İstanbul, 945-953.